
Microscopic Observations of Needle-Tissue Interactions

Auke Been

BSc project

Supervisors:

prof.dr.ir. S. Stramigioli
dr. S. Misra
dr.ir. N.R. Tas

March 2011

Report nr. 004CE2011
Control Engineering
EE-Math-CS
University of Twente
P.O. Box 217
7500 AE Enschede
The Netherlands

Abstract

This report focusses on the design, construction and testing of a new set-up which is designed to observe needle-tissue interaction. A model to describe interactions between a needle and tissue is being made and needs physical observations for further development. The key features of the set-up are that it is able to observe needle insertion under a laser scanning confocal microscope and that the set-up can measure the six forces and torques that occur during insertion. The set-up was designed based on a set of requirements and constructed using several prefabricated parts. The results show that the set-up is efficient up to at least 1 mm/s insertion velocity and twenty times microscope magnification.

Contents

1	Introduction	4
2	Method	4
2.1	Confocal microscope	4
2.2	Set-up requirements	5
2.3	Set-up design	5
2.4	Measurement method	6
2.5	Post-processing of results	8
3	Results	8
3.1	Tissue Interaction Images	9
3.2	Needle: 19G Speed: 0.1 mm/s Case: 2	10
3.3	Needle: 23G Speed: 0.1 mm/s Case: 2	11
3.4	Needle: penelope200x400 Speed: 0.1 mm/s Case: 1	12
3.5	Needle: 21G Speed: 0.5 mm/s Case: 2	13
3.6	Needle: 27G Speed: 0.5 mm/s Case: 3	14
3.7	Needle: 30G Speed: 1 mm/s Case: 1	15
3.8	Needle: penelope400x400 Speed: 1 mm/s Case: 2	16
4	Discussion	17
4.1	Observations	17
4.2	Relating Graphs to Images	18
4.3	Shearing	18
4.4	Dark lines	18
4.5	Needle bending	18
4.6	Microneedles	18
4.7	Higher insertion speeds	18
5	Conclusion	19
6	Recommendations	19
7	Acknowledgments	19
8	Scientific Output	19
	Appendices	20
A	Mechanical Drawings	20
B	Results	30

1 Introduction

Minimally invasive procedures using needles are frequently used for treatment and diagnosis. As the needle is inserted deeper into the body, deflection of the needle occurs and hinders the physician in working effectively. To attain more insight in the deflection of the needle, a model has been developed to describe the forces on the needle [1]. The ultimate goal of this model is to use it to be able to steer needles using a robot and make procedures involving needles accurate and precise by enabling the needle to reach the intended target in one try. The modelling will benefit from precise observations of needle-tissue interactions during insertion, for which a set-up will have to be created. The scope of this assignment was to design, construct and test a set-up which will allow us to observe these interactions.

In the Method section, the confocal microscope is described as well as the set-up requirements, set-up design, measurement method and the processing of the results. The results are presented in the Results section together with the required settings on the equipment. The presented results will be discussed in the Discussion section, followed by the conclusions in the Conclusion section. The Recommendations, Acknowledgements, References and Scientific output sections finalize the report.

2 Method

In this section, we will focus on the confocal microscope, the design and construction of the set-up, the measurement method and the processing of the results.

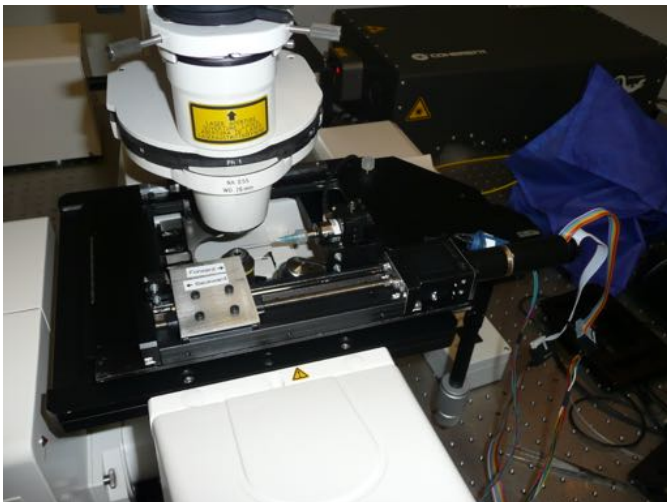


Figure 2.1: The LSM with the set-up installed on the XY-table. The stainless steel carriage can be seen on the left-hand side of the set-up. This moves over the objective, under the XY-table. The needle on the right side of the set-up is attached to the force sensor. Above the set-up is another part of the microscope, which picks up the transmitted light.



Figure 2.2: The Zeiss LSM 510 of the Nanobiophysics group at the University of Twente. The set-up which is described in this report is already installed on the XY-table of the microscope. The objective is located under the XY-table. The structure above the XY-table is used to illuminate the specimen in ocular mode and to pick up the transmitted light images while in laser scanning mode.

2.1 Confocal microscope

To observe the rupturing process during needle penetration of tissue, we will be using a laser scanning confocal microscope (LSM). In order to observe what happens inside a tissue at this scale, the confocal microscope is ideal. Its ability to show only the plane of focus is perfect for our application. Unfortunately LSM microscopes are not capable of taking images at high framerates. This is not a problem at low insertion velocities, but we will lose information at higher insertion velocities. The Zeiss LSM 510 will be used for the experiments, as it is readily available at the University of Twente. A photograph of the microscope, already with the set-up installed, is shown in figure 2.1 and figure 2.2. Note that the lens is below the specimen and thus focuses from below. The structure above the XY-table (the XY-table is the moveable stage of the microscope itself and does not refer to the coordinate system which will be used later in the report) is for lighting the specimen homogeneously in ocular mode and for picking up the transmitted light images; that is it picks up the light that has passed through the sample while in laser scanning mode.

A diagram of confocal microscopy is shown in figure 2.3 and shows how the principle works [2]. The laser shines light on the specimen. Reflected light is split by a dichroic

beam splitter and is then filtered by an aperture, which allows us to select only the z-plane that is in focus. The thickness of the slice that is detected depends on the size of the aperture. In the Zeiss LSM 510, there is also a detector on the other side of the specimen which picks up the light that passes through the specimen. There is also a filter after the beamsplitter that filters light above a certain wavelength. The confocal part of the Zeiss microscope works with fluorescence. We will be using the fluorescent dye FITC (fluorescein-5-isothiocyanate from invitrogen) in our specimen to see where the needle is. As the needle is not fluorescent, it can be distinguished from the rest of the specimen. FITC has an excitation wavelength of 495.0 nm and an emission wavelength of 519.0 nm[3]. The filter after the beamsplitter should filter the excitation wavelength and only allow the emitted light by the fluorescent dye through. This prevents excitation light reflected by the needle to reach the detector.

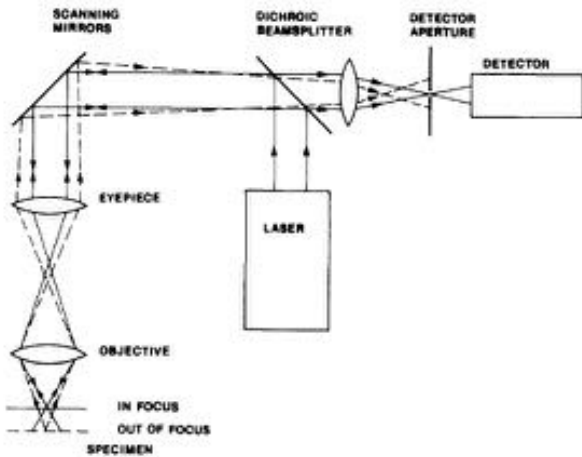


Figure 2.3: Diagram of the confocal principle. A laser shines light on a specimen. The reflected light goes through a beamsplitter and is filtered by an aperture, which allows confocal microscopes to filter out of focus regions.

2.2 Set-up requirements

In order to observe the needle insertion at all under the microscope, we will need a set-up that can hold a needle, a specimen and have them move to achieve an insertion. The focus of this assignment was to design, construct and test this set-up. The primary requirements for constructing such a set-up are listed here. They are:

- Hold a needle
- Hold a specimen
- Have them move to achieve insertion
- Measure the forces in this interaction between needle and tissue
- Move at user determined speeds
- Fit within the confines of the confocal microscope

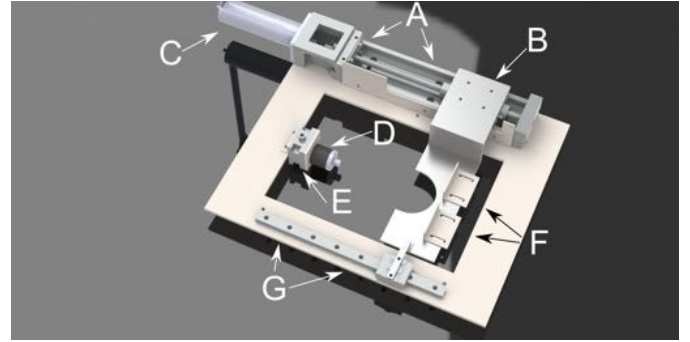


Figure 2.4: SolidWorks (DS SolidWorks, Concord, Massachusetts, VS) model of the set-up. The linear actuator (A) is driven by the EC-motor (C) and enables the carriage (B), that will be holding the specimen, to move. The other side of the carriage is held up by a linear guide (G), to prevent vertical movement and bending of the carriage. Mounted on the carriage are two braces (F) to hold the specimen in place. Finally there is an adjustable stage (E) mounted on the base plate to mount the force sensor (D) on.

2.3 Set-up design

The design includes a few prefabricated parts to optimize precision and assembly speed. An image of the final design is shown in figure 2.4. The base plate will be mounted on the XY-table of the microscope. In order to keep the needle in the image of the confocal microscope, we have decided to fix the needle at one point and have the specimen move 'over' the needle to achieve insertion. This way the needle tip will always be in view of the microscope. To drive the specimen, we use a linear actuator which is powered by an electrical motor. The specimen rests below the XY-table in order to have the specimen within the focal reach of the lens. The specimen is held in place by two brackets that prevent movement in the insertion direction. The lens is able to observe what occurs within the specimen through the hole cut in below the specimen and between the two brackets. On the other side of the carriage that holds the specimen a linear guide is installed. This keeps the structure steady and prevents vertical movement and bending. The compliance of the part that connects the linear guide and the carriage is chosen such that movement is not restricted while still supporting the carriage. All the mechanical drawings for the set-up can be found in Appendix A.

The linear actuator is driven by a Maxon EC-max motor (maxon motor benelux bv, Enschede, The Netherlands). This motor is electronically commutated by a separate controller. We have chosen for the ELMO whistle (Elmo Motion Control Ltd., Petach-Tikva, Israel) controller because there is already a lot of experience using this controller in the Control Engineering group as well as for its ability to commutate the motor with sinusoidal signals. The advantage of a sinusoidal commutation is that it allows us to regulate the speed more accurately over a wide range of velocities. The controller can be given commands through a simple serial interface by a computer.

The needle is held by a linear stage and a force sensor. The height of the needle with respect to the specimen can

be adjusted with the linear stage. Each lens has a certain maximal focus distance and because we will be testing needles of various sizes, we want to be able to adjust the height of the needle. Generally speaking the needle needs to be as close to the bottom of the specimen as possible, but not so close as to touch the glass or see effects of the interface between the gel and the glass. In the experiments we tried inserting the needle about 1 mm above the glass. If the needle is too close to the glass, edge-effects of the tissue might occur, in which we are not interested.

We have considered several kinds and brands of force sensors. We expect the forces involved in needle-tissue interactions are below 1 N: results based on needle insertions into pork skin show forces upto 0.8 N [4]. The force sensor will have to be able to measure forces well below this 0.8 N. In the end we have chosen for the ATI Nano 17 (ATI Industrial Automation, Apex, VS), which is able to measure forces and torques along the three axes. In Table 2.1 the sensing range and resolution of the Nano 17 is listed. The resolution can be further increased by averaging measurements:

$$\epsilon = \frac{\sigma}{\sqrt{N}}$$

Where ϵ is the error, σ is the standard deviation and N the amount of samples that are averaged. The forces and torques can be read with a data acquisition card in a PC. Because the sensor is quite fragile, the connection between the needle and the sensor is made with magnets. Using magnets allows for an easy system to replace needles and decreases the chance that the sensor is rendered useless by applying too much force on the sensor during a change of needles. The needles are held by a global standard Luer twist lock which can mount any needle as long as the needle is held in the global standard needle base.

	Sensing range	Resolution
F_x, F_y	12 N	1/320 N
F_z	17 N	1/320 N
T_x, T_y	120 N mm	1/64 N mm
T_z	120 N mm	1/64 N mm

Table 2.1: Sensing range and resolution of the Nano 17 along the different axes.

To control the whole set-up a LabView Virtual Instrument (VI) has been designed. In this VI communication with the controller is managed and the readings from the force/torque sensor saved. Because the output wire of the sensor was placed in an optimal position with respect to the XY-table of the microscope, the axes of the set-up and the sensor do not line up. A coordinate system transformation in the VI takes care of this using Equation 2.1 and saves a file in the coordinate system of the set-up itself.

$$\begin{aligned} x &= x_{sensor} \cos(30^\circ) - y_{sensor} \cos(60^\circ) \\ y &= x_{sensor} \sin(30^\circ) + y_{sensor} \sin(60^\circ) \\ z &= z_{sensor} \end{aligned} \quad (2.1)$$

Here the x , y and z represent the coordinates in the desired coordinate system. x_{sensor} , y_{sensor} and z_{sensor} represent the coordinates that the force sensor uses. The x-axis of

the sensor is mounted under an angle of 30° with respect to the desired x-axis.

The readings of the force/torque sensor are acquired with a data acquisition card of National Instruments: NI PCI-6035E. The VI acquires 2000 samples, which are averaged to increase accuracy, every 100 ms.

The construction of the set-up took a long time due to delays in the ordering and delivery of the EC-motor and the ATI Nano 17. With a total delay of just over four months the set-up was finished six months after the start of the project.

2.4 Measurement method

To provide proof that the set-up really works as required, we performed several experiments. We decided to test 7 different kinds of needles at 3 different insertion speeds in triplo. The needles that we will be using are 5 standard issue hypodermic needles, 19G, 21G, 23G, 27G and 30G, and 2 experimental microneedles, the penelope $200 \mu\text{m} \times 400 \mu\text{m}$ and $400 \mu\text{m} \times 400 \mu\text{m}$, provided by microneedle (Enschede). These needles are shown in figure 2.5.

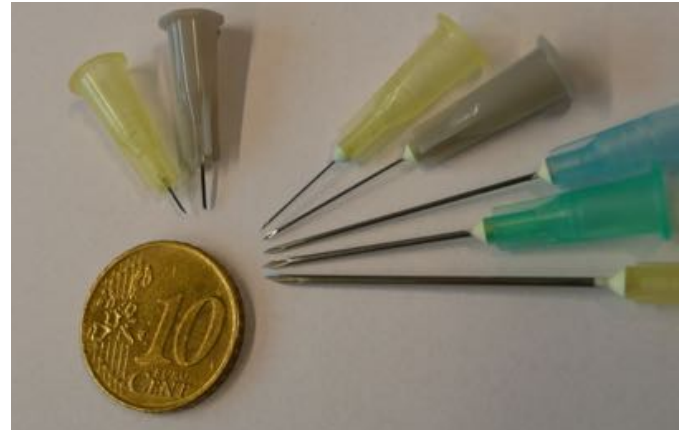


Figure 2.5: Image of all the needles used in our experiments. From left to right: Penelope $200 \mu\text{m} \times 400 \mu\text{m}$, Penelope $400 \mu\text{m} \times 400 \mu\text{m}$, 30G, 27G, 23G, 21G, 19G.

The dimensions of the hypodermic needle shafts are listed in Table 2.2.

Needle	Size	Tolerance
19G	$1067 \mu\text{m}$	$\pm 13 \mu\text{m}$
21G	$819.2 \mu\text{m}$	$\pm 6.4 \mu\text{m}$
23G	$641.4 \mu\text{m}$	$\pm 6.4 \mu\text{m}$
27G	$412.8 \mu\text{m}$	$\pm 6.4 \mu\text{m}$
30G	$311.2 \mu\text{m}$	$\pm 6.4 \mu\text{m}$

Table 2.2: The dimensions of the shafts of hypodermic needles as specified by the International Organization for Standardization. [5]

We define the axes of the system as follows: The graphs show the forces and torques along the 3 axes, which are shown in figure 2.6

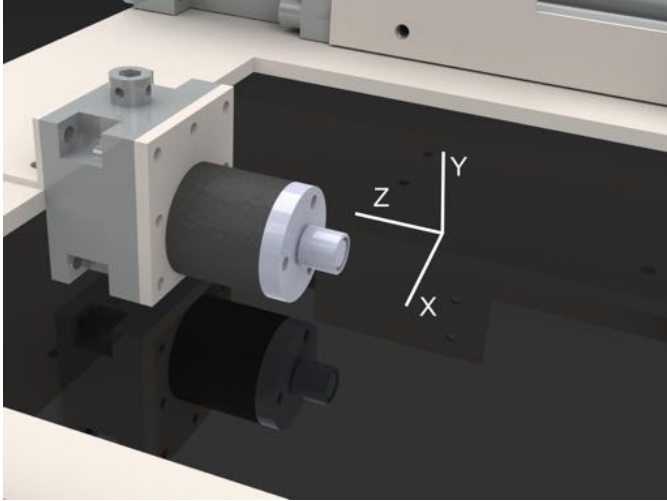


Figure 2.6: Image of a part of the set-up to show the coordinate system: x horizontal and perpendicular to the needle, y vertical and perpendicular to the needle and z parallel with the needle. The needle is to be mounted on the end of the cylindrical objects.

We will save force readings and microscope images during the insertion as well as a stack for 3D reconstruction of the needle¹ after insertion and a normal image of the gel after retracting the needle. Because real tissue requires an elaborate and expensive protocol, we have decided on using agarose gel as a replacement. The agarose gel is easily made, easy to come by and the density is easily changed according to the amount of added agarose powder to the solution. Agarose powder from the manufacturer Sigma (Product # A9539) was used. The procedure of making an 2 % agarose gel is as follows:

1. Add 2 mg agarose to 100 mL 1x Tris-acetate (TAE).
2. Heat the suspension in the microwave to boiling point.
3. Swirl the mix until the agarose is completely dissolved and the solution is clear.
4. Add 1 mL fluorescein-5-isothiocyanate-protein conjugate (FITC), fluorescent dye, to the solution. This is essential for the microscope to observe anything from the confocal channel.
5. Pour the solution in a mold and let it cool down until the solution has solidified.

50x TAE is made using the following procedure, this can be diluted to 1x with H_2O as required:

1. Dissolve 242 g Tris² in 500 ml H_2O .
2. Add 100 ml 0.5 M Na_2EDTA ³ (pH 8.0) and 57.1 ml glacial acetic acid.
3. Adjust volume to 1 liter with H_2O .
4. Store at room temperature.

¹This is called a z-stack in the microscope software, in our coordinate system it would be a y-stack

²tris(hydroxymethyl)aminomethane

³EDTA stands for Ethylenediaminetetraacetic acid

After installing the set-up on the XY-table of the microscope, the measurement procedure was as follows:

1. Mount a needle on the Luer lock and place it on the sensor, making sure the tip of the needle is in the x -plane. During insertion the needle will bend due to forces on the tip. Having the tip in the xz -plane will prevent the needle from bending out of focus. This is shown in figure 2.7
2. Align the needle to the gel with the linear stage using a hex key. Take care to place the needle within the focal 'reach' of the lens, but not too close to the bottom of the gel where it will cause the gel to tear from the glass.
3. Insert the needle in to the gel and select the right settings for the microscope; focus and gain. Also take in consideration that the needle will bend and that it could move out of the image. Select the range of foci for the z -stack. Because the gel has a different refractive index than air, it is important to find the focus inside the gel rather than outside.
4. Retract the needle and position the gel for a new insertion. Move the carriage such that the gel is just before the tip of the needle.
5. Start the timelapse of the microscope and start the VI to record the force/torque measurements and initiate the movement of the gel.
6. After the desired distance has been travelled, the controller will automatically stop the motion. The timelapse of the microscope will have to be stopped manually.
7. Take a z -stack reading with the microscope.
8. Retract the needle and position it for a new measurement.
9. Repeat steps 5 to 8 for the different desired measurements with the same needle.
10. Take images of what the needle left behind after retraction of the needle. Because the position of the XY-table has to be adjusted for this, all the insertions are done first. This eliminates the need to repeat steps 3 and 4 after each insertion.

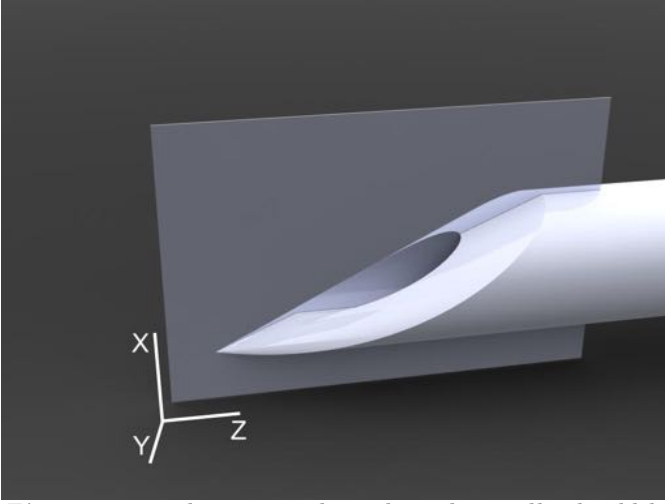


Figure 2.7: This image shows how the needle should be aligned with the axes. To avoid movement of the tip in the y direction, the tip should be completely in the xz -plane such that the plane cuts the needle perfectly in half.

2.5 Post-processing of results

The Labview VI outputs a comma separated value file, which needs to be processed for efficient processing. After a script processes the files, gnuplot (version 4.2, open source plot environment, www.gnuplot.info) can create graphs of the force and the torque. The script applies the following steps:

- Add column headers for gnuplot
- Bias all readings with the first reading: $\text{sample}[n] = \text{sample}[n] - \text{sample}[0]$
- Add a column for the relative position of the specimen with respect to the needle. The VI will record samples during a certain timespan. This is a programmed $t = \frac{d}{v}$, where d is the displacement, v the velocity and t the time. To this calculated time a programmed 3s is added to be able to observe the forces and torques as the specimen relaxes after insertion. There is also an unknown amount of samples recorded before the motor is turned on. This is due to a delay that can not be circumvented, because the recording of forces and torques is started before the motor starts. This results in several force and torque readings before the countdown timer is started.

3 Results

The following pages show a few of the measurements mentioned above. All measurements can be found in Appendix B. In Table 3.1 shows which measurements are presented in the section.

Case	Needle	Speed
2	19G	0.1 mm/s
2	23G	0.1 mm/s
1	penelope 200×400	0.1 mm/s
2	21G	0.5 mm/s
3	27G	0.5 mm/s
1	30G	1 mm/s
2	penelope 400×400	1 mm/s

Table 3.1: Overview of the experiments of which the results are presented in this section

Each measurement will be presented on its own page, displaying graphs of the forces and torques, the time series, inverse 3-D reconstruction and an image showing the insertion path after the needle was retracted. Note that all the images show a scalebar of 100 μm

All experiments were done using the following settings:

- Objective: Plan-Neofluar 20x/0.5⁴
- Filter: LP 560
- Beam splitters: HFT 488
- Laser: 488 nm, 6.0 %

All needles will be moved over a distance of 5 mm, except for the micro needles, which are shorter. The micro needles are only moved 3 mm.

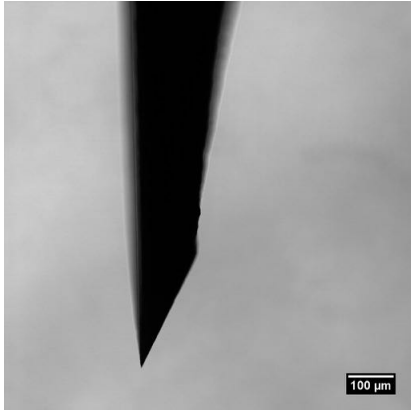
The time series images show recorded times. As the microscope takes two seconds to scan one image, we can easily work out the time that has passed after the first scan. With the time from the image when the needle enters the gel and the velocity of the insertion, we can work out the travelled distance to correlate to the graphs. We have chosen not to do this for these results, as these experiments are only to show that the set-up works.

All the images taken by the LSM are in the same plane as the plane shown in figure 2.7, though in some experiments the needle was rotated 180°.

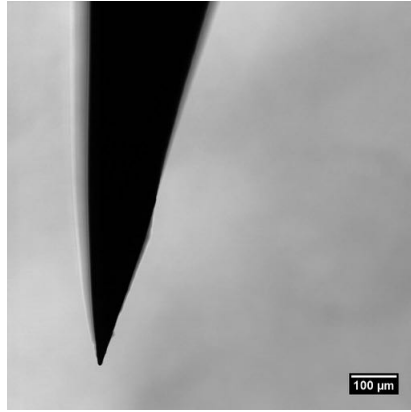
⁴Larger magnification will result in the needle bending out of the field of view.

3.1 Tissue Interaction Images

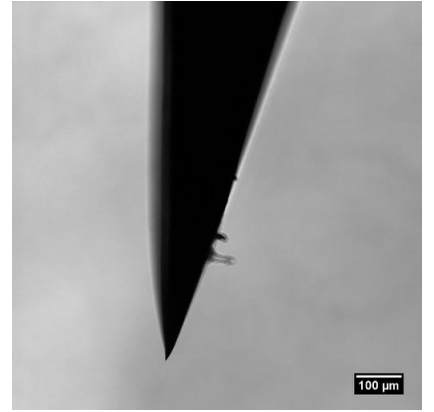
In figure 3.1 the needles that were used are shown as they were scanned by the microscope outside the gel. Note that the shape of the needles differs a lot. We used the same needle for all experiments of that needle type, so that the results can be compared with each other.



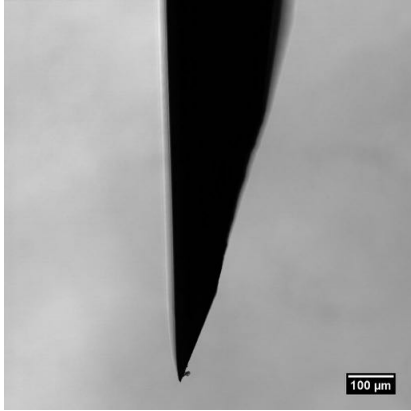
(a) The 19G needle



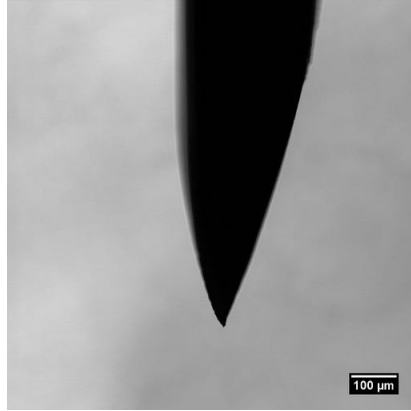
(b) The 21G needle



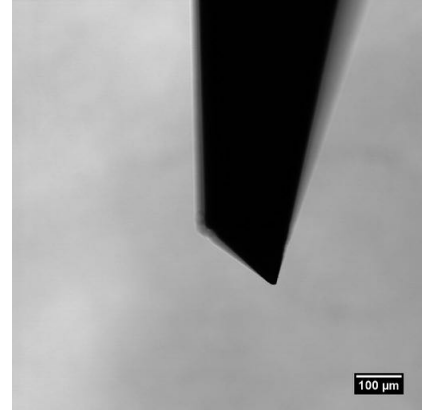
(c) The 23G needle



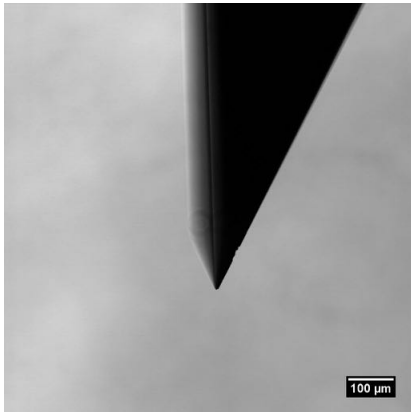
(d) The 27G needle



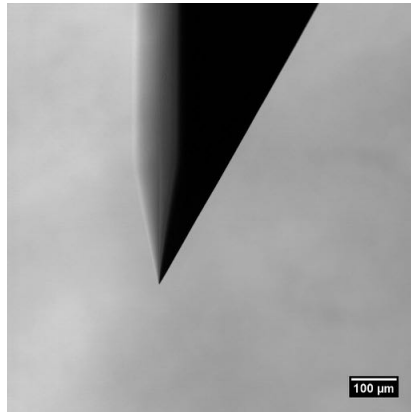
(e) The 30G needle



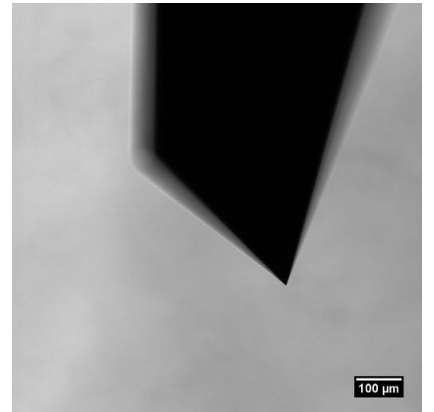
(f) One face of the penelope 200 μm × 400 μm needle.



(g) Another face of the penelope 200 μm × 400 μm needle.



(h) One face of the penelope 400 μm × 400 μm needle.



(i) Another face of the penelope 400 μm × 400 μm needle.

Figure 3.1: The different needles that were used in our experiments. These images were taken using the Plan-Neofluar 10x/0.3 objective.

3.2 Needle: 19G Speed: 0.1 mm/s Case: 2

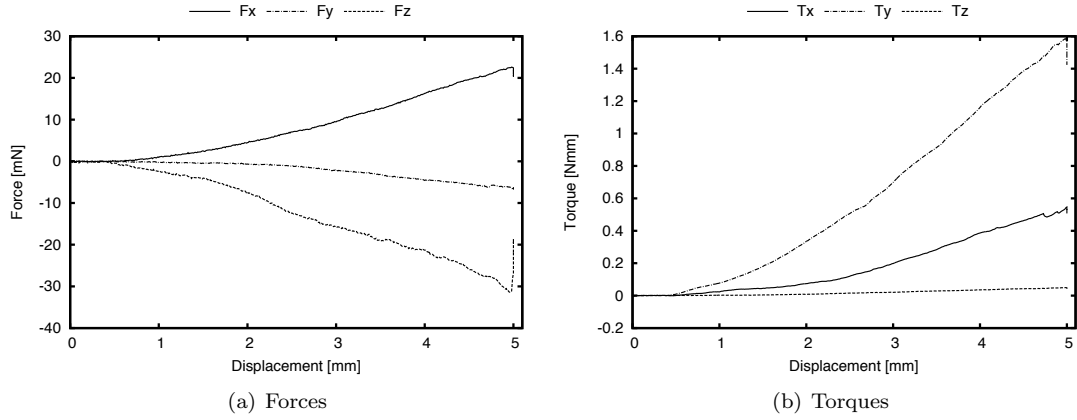


Figure 3.2: The forces and torques recorded with the ATI Nano 17.

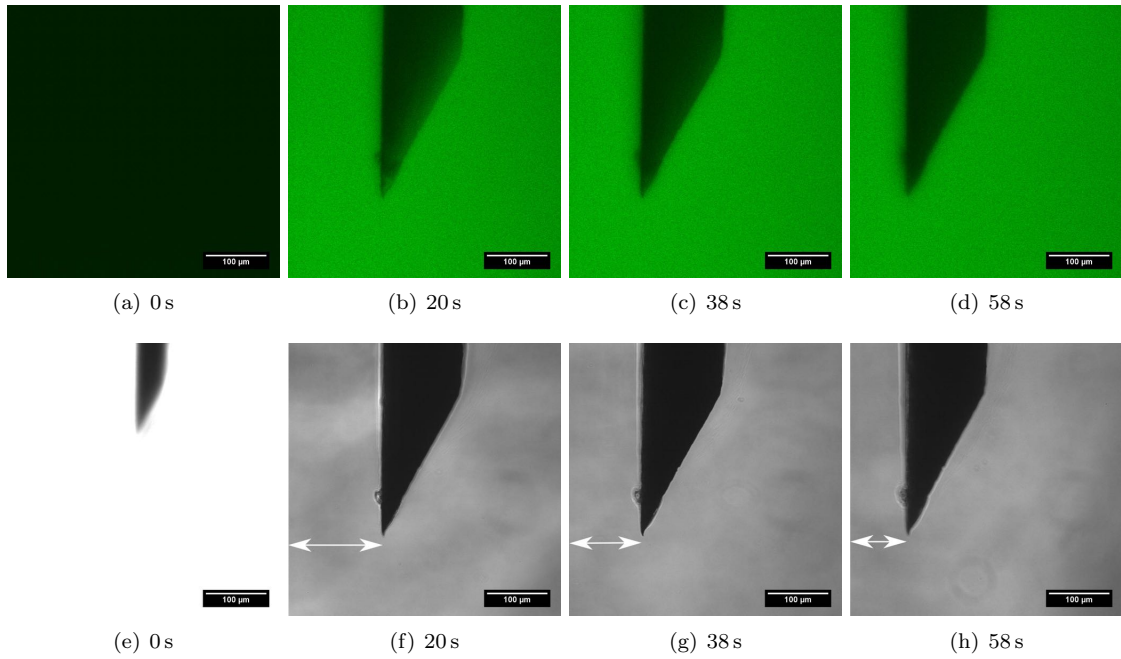


Figure 3.3: a-d show the confocal fluorescent images taken with the LSM, e-h show the transmitted light images. The arrows clearly show the needle moving to the left as it was inserted.

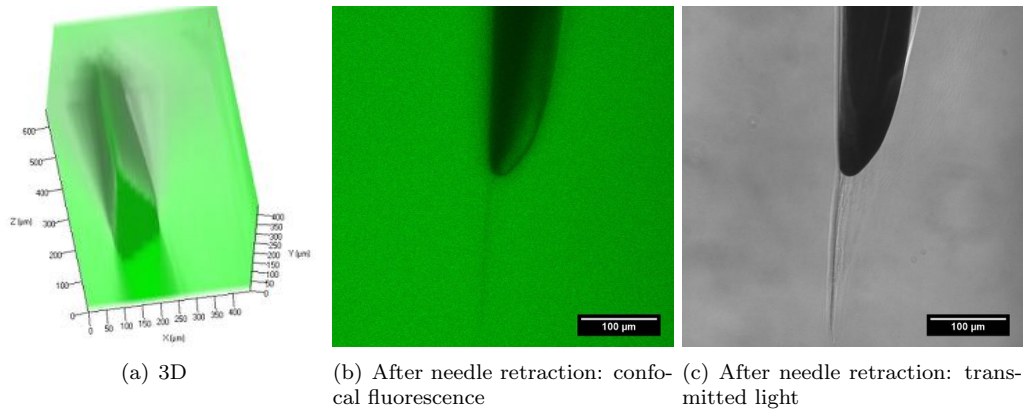


Figure 3.4: Images showing 3-D reconstruction before needle retraction and normal images after retraction.

3.3 Needle: 23G Speed: 0.1 mm/s Case: 2

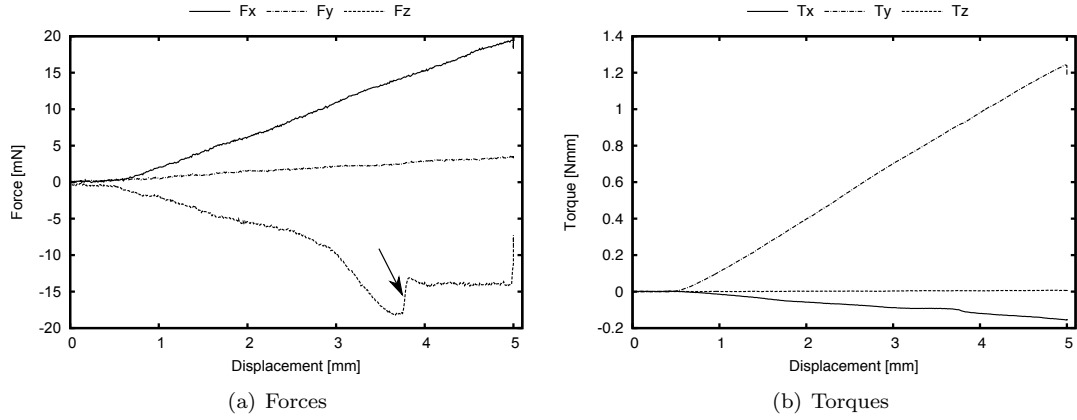


Figure 3.5: The forces and torques recorded with the ATI Nano 17. The arrow points at a bump which was recorded in every experiment with this needle.

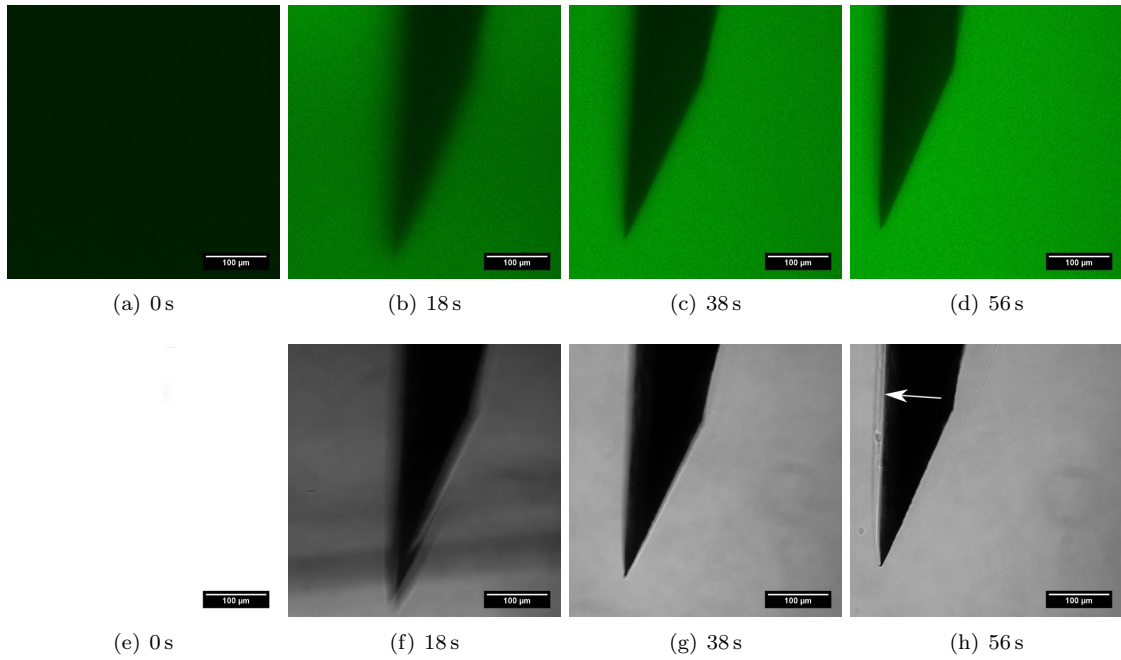


Figure 3.6: a-d show the confocal fluorescent images taken with the LSM, e-h show the transmitted light images. The arrow shows deformation of the gel after the movement stopped and the system relaxed.

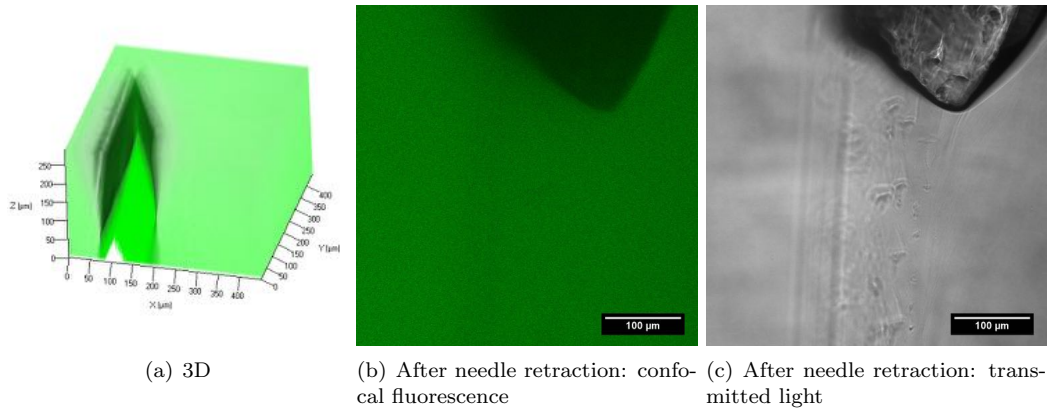


Figure 3.7: Images showing 3-D reconstruction before needle retraction and normal images after retraction.

3.4 Needle: penelope200x400 Speed: 0.1 mm/s Case: 1

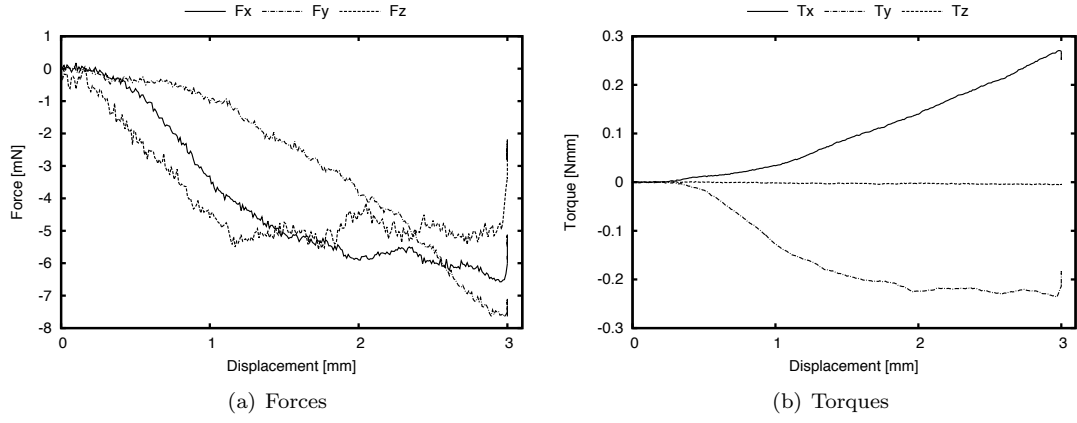


Figure 3.8: The forces and torques recorded with the ATI Nano 17.

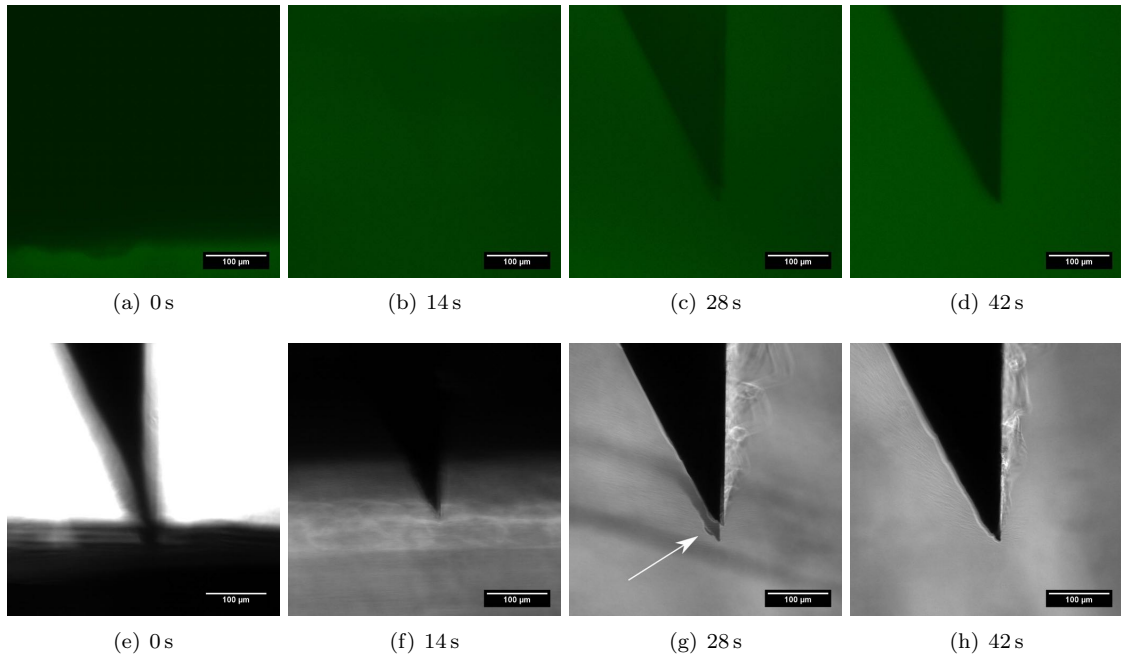


Figure 3.9: a-d show the confocal fluorescent images taken with the LSM, e-h show the transmitted light images. The arrow points at a shadow caused by a sudden movement of the needle.

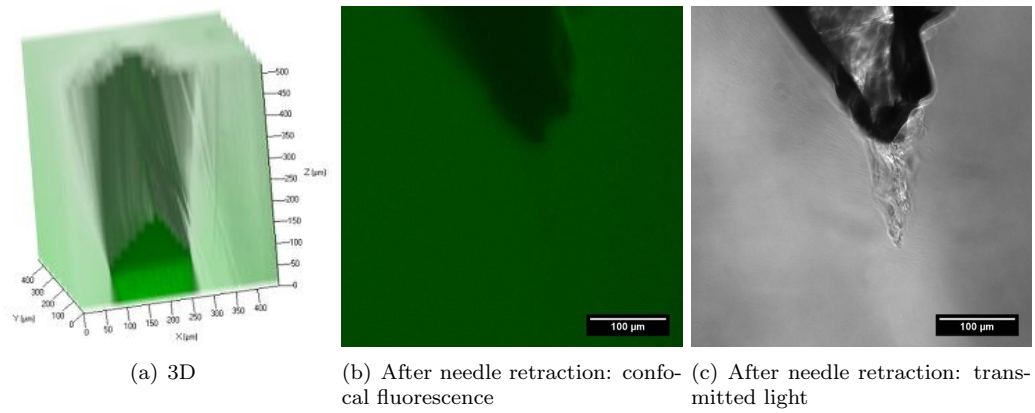


Figure 3.10: Images showing 3-D reconstruction before needle retraction and normal images after retraction.

3.5 Needle: 21G Speed: 0.5 mm/s Case: 2

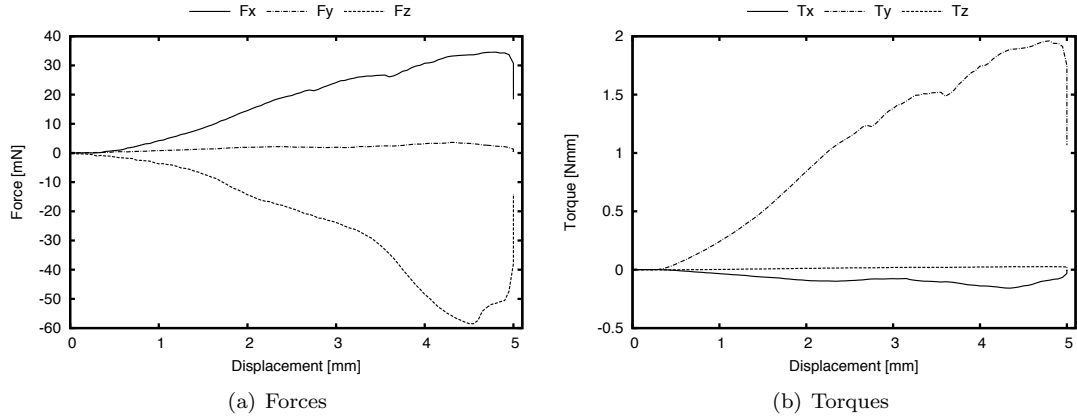


Figure 3.11: The forces and torques recorded with the ATI Nano 17.

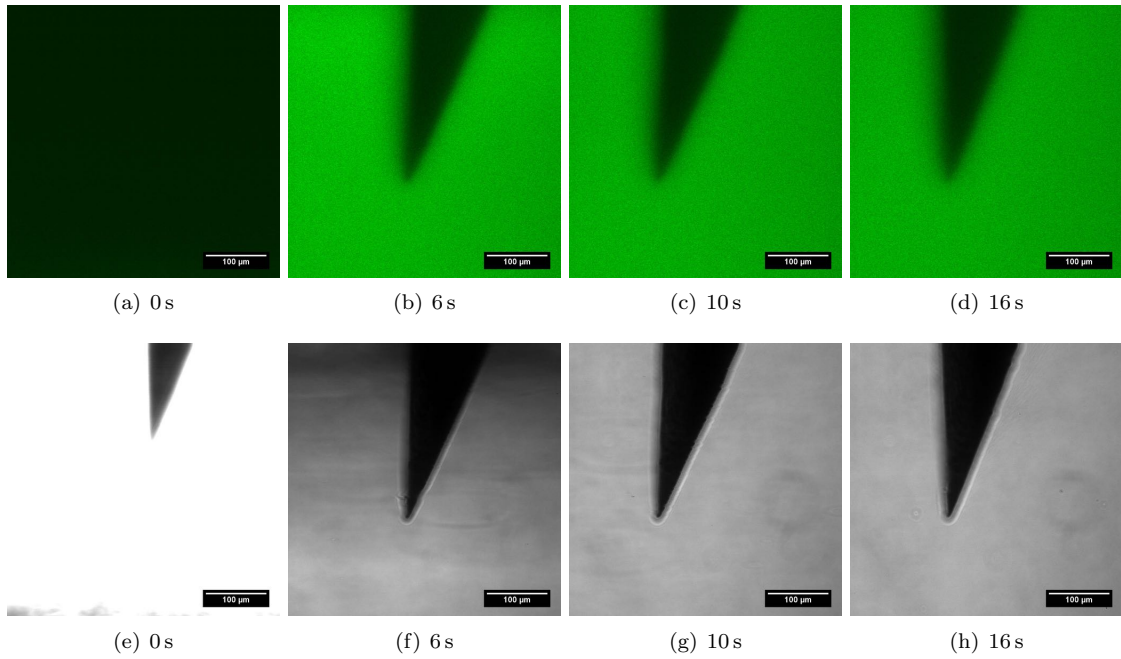


Figure 3.12: a-d show the confocal fluorescent images taken with the LSM, e-h show the transmitted light images.

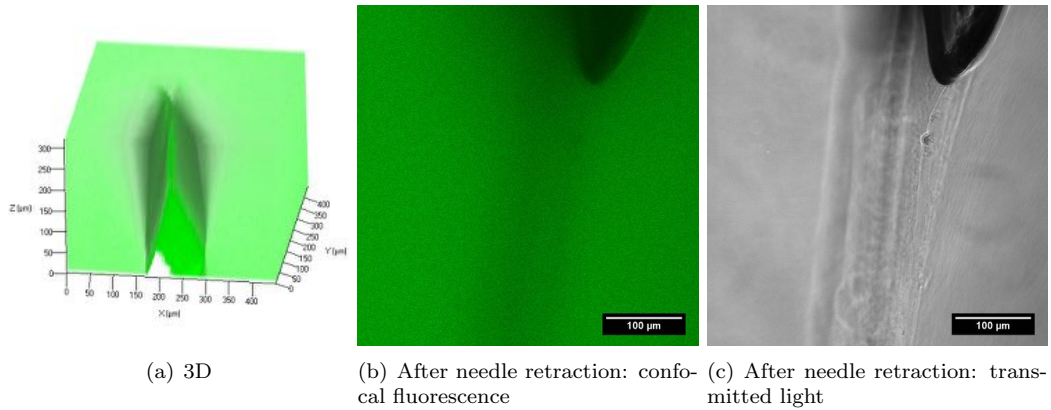


Figure 3.13: Images showing 3-D reconstruction before needle retraction and normal images after retraction.

3.6 Needle: 27G Speed: 0.5 mm/s Case: 3

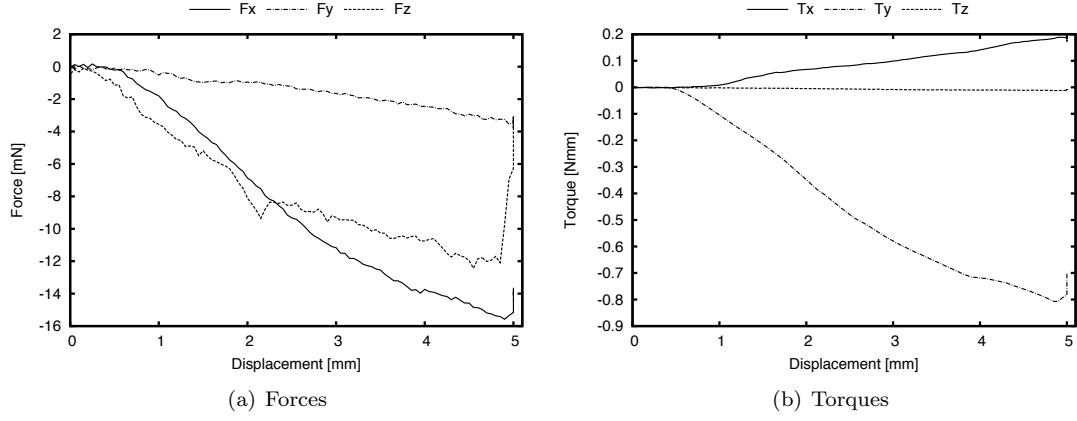


Figure 3.14: The forces and torques recorded with the ATI Nano 17.

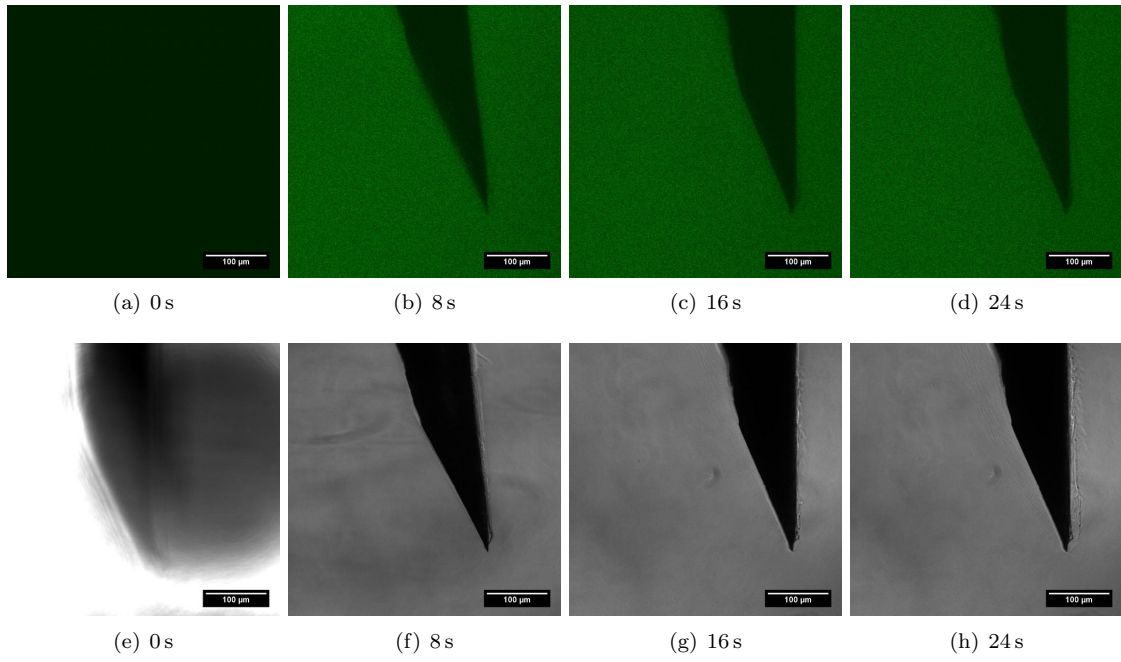


Figure 3.15: a-d show the confocal fluorescent images taken with the LSM, e-h show the transmitted light images.

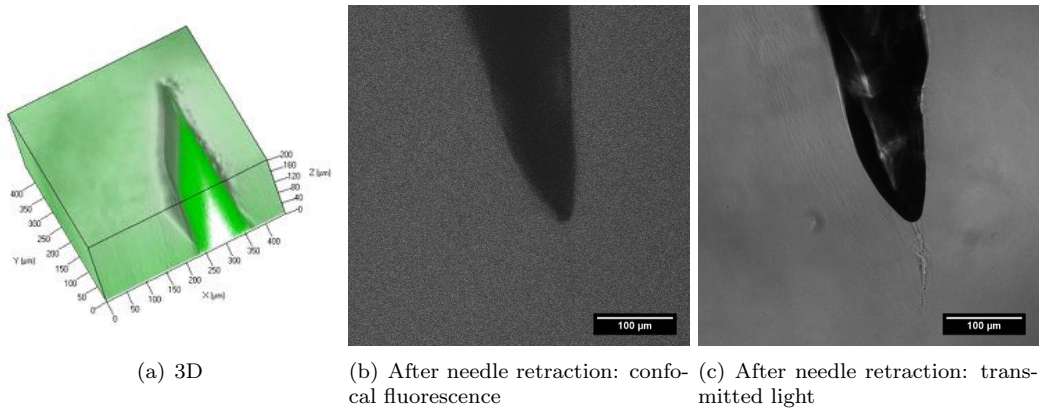


Figure 3.16: Images showing 3-D reconstruction before needle retraction and normal images after retraction.

3.7 Needle: 30G Speed: 1 mm/s Case: 1

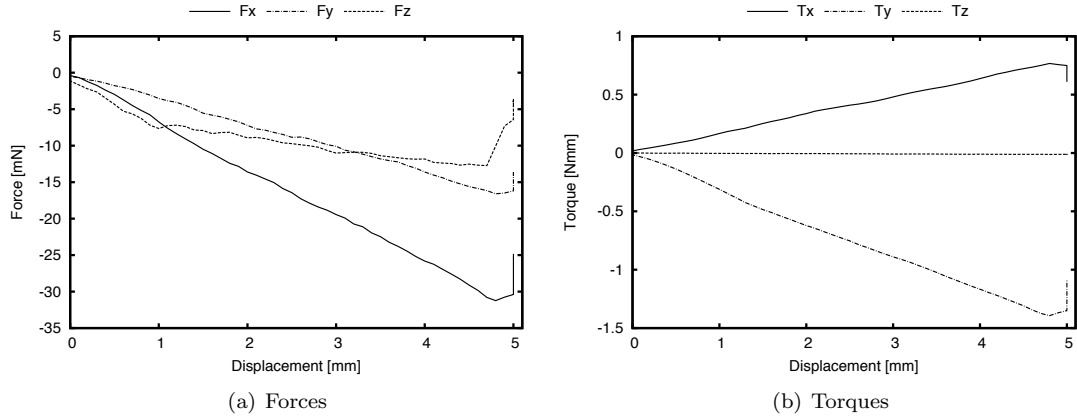


Figure 3.17: The forces and torques recorded with the ATI Nano 17.

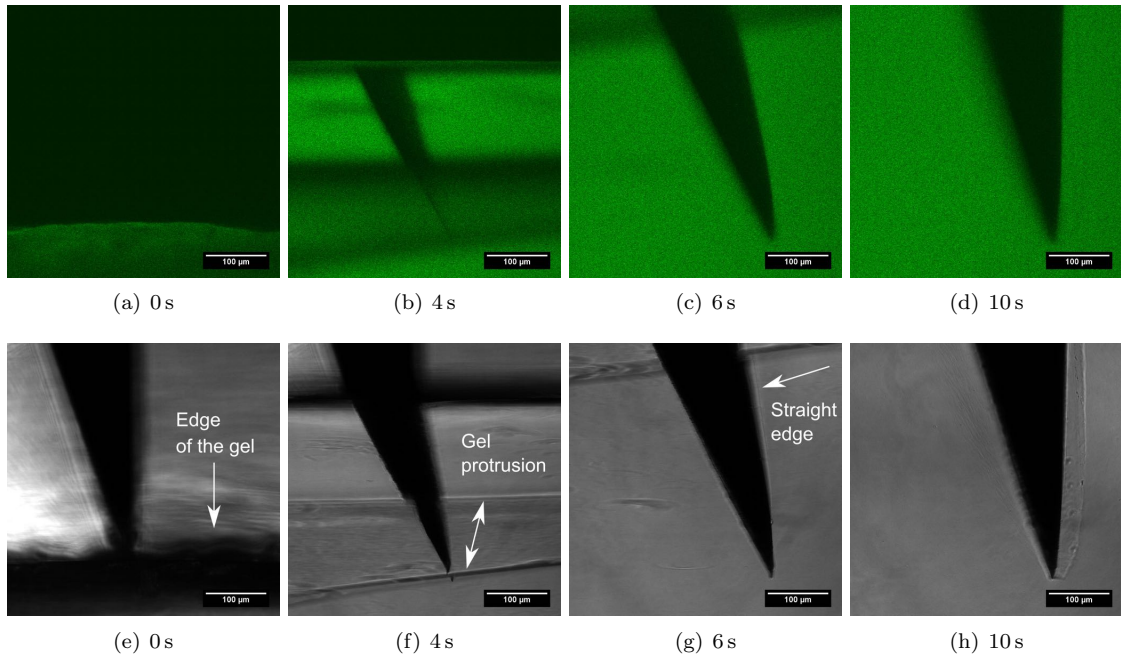


Figure 3.18: a-d show the confocal fluorescent images taken with the LSM, e-h show the transmitted light images. The arrows in images e and f point at anomalies in the gel. The arrow in image g shows the effect of laser scanning on the imaged straightness of the needle.

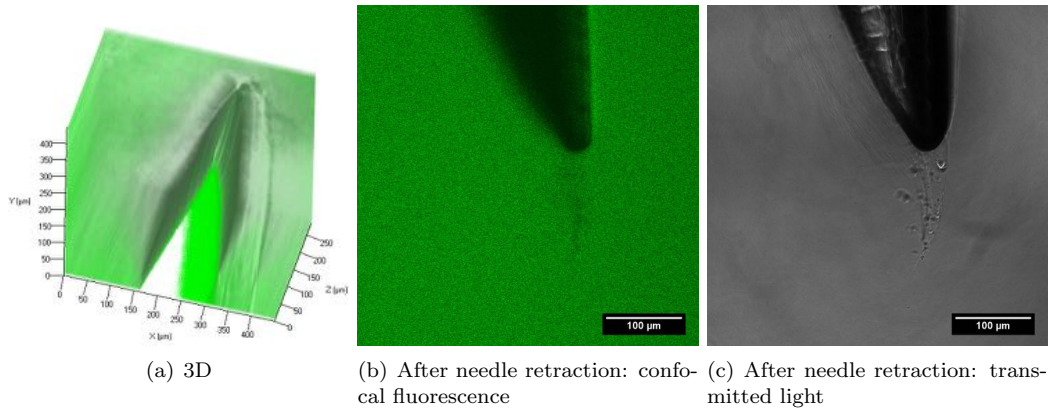


Figure 3.19: Images showing 3-D reconstruction before needle retraction and normal images after retraction.

3.8 Needle: penelope400x400 Speed: 1 mm/s Case: 2

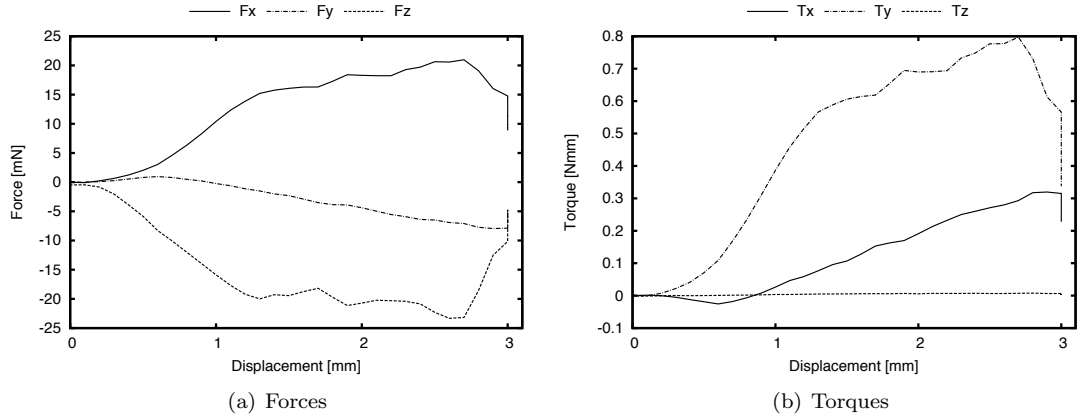


Figure 3.20: The forces and torques recorded with the ATI Nano 17.

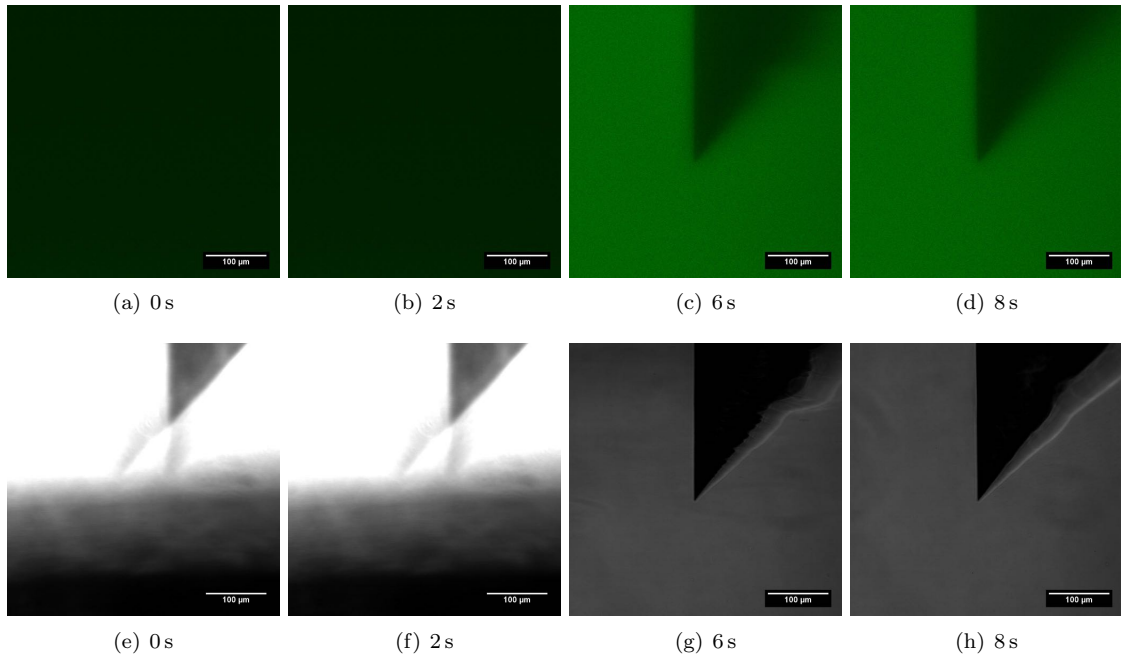


Figure 3.21: a-d show the confocal fluorescent images taken with the LSM, e-h show the transmitted light images.

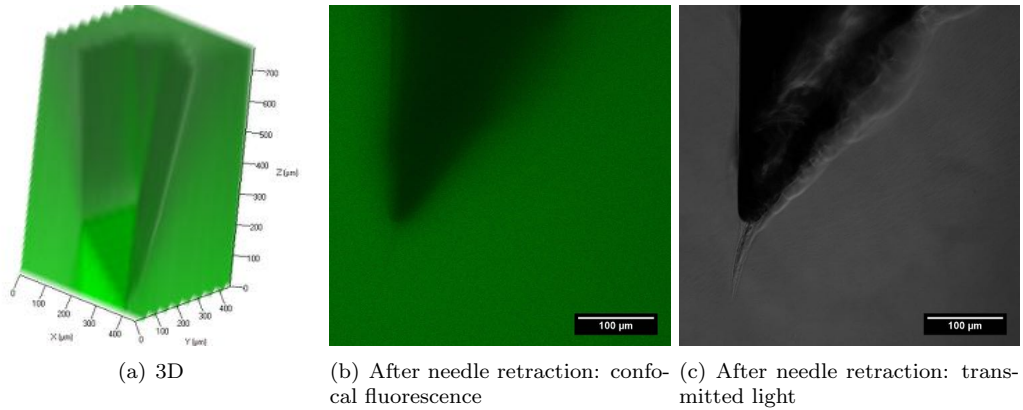
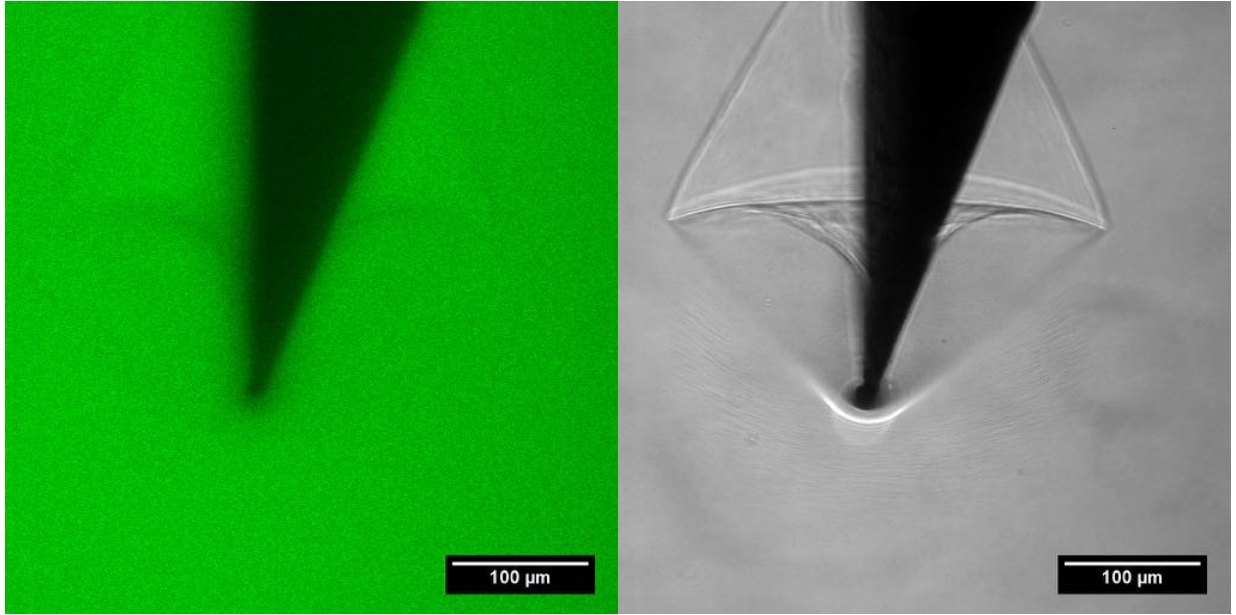
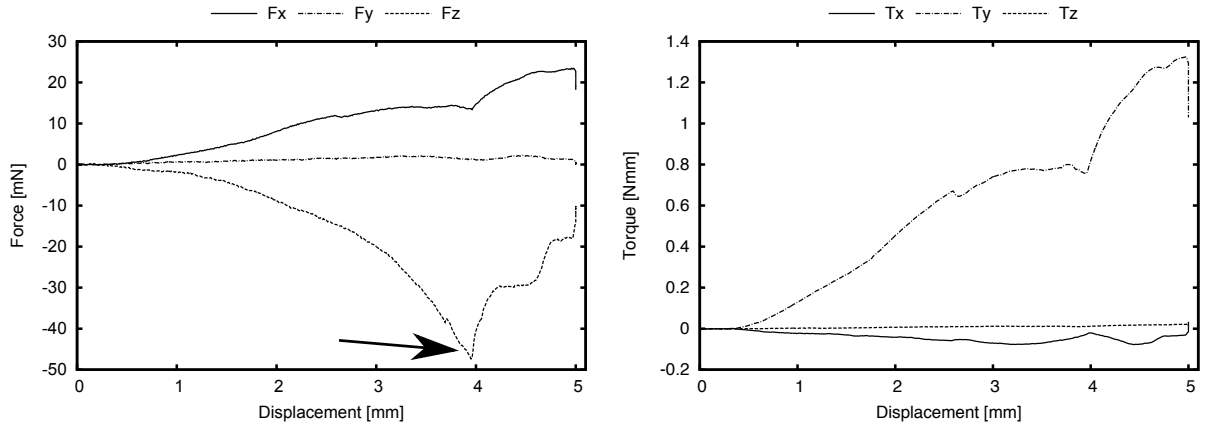


Figure 3.22: Images showing 3-D reconstruction before needle retraction and normal images after retraction.



(a) Microscope images



(b) Force and Torque graph of the same measurement

Figure 3.23: Images showing shearing close to the glass and the corresponding force and torque graphs. The confocal fluorescence image does not show the shearing very clearly because this phenomenon was out of the plane of focus. This image is one of the 0.1 mm/s 21G-2 measurement at 28 s and corresponds with the graphs at about 2.8 mm insertion. The needle finally punctured the shear and continued normal insertion at 4 mm insertion, which corresponds to about 40 s. The arrow points at the peak which corresponds with the puncture of the shearing.

In figure 3.23 shearing of the gel occurs on the interface with the object slide. This was observed with several needles when they were inserted too close to the glass.

4 Discussion

In the following section the results will be discussed. First general observations will be outlined, after which we will discuss some observations in more detail.

4.1 Observations

First of all looking at the graphs of the measurements in Appendix B, they show that the results are reproducible: the general impression is that the measurements with the same needle and velocities have the same results. Also notice that the forces of the same needle, but at higher insertion speeds increase — as one would expect.

The graph shown in figure 3.2 is one as we would expect. Initially no forces or torques were recorded as the initial gap between the needle and the gel was travelled by the needle. After that the F_z increased as the needle was inserted deeper into the gel. There was also an increase in the F_y and a slight increase in the F_x . These are due to the bending of the needle. As the needle bent it produced forces and moments, which are shown in the graphs. This bending was also observed in the torque T_x and T_y . Carefully observing the time series images, one can also see the bending as it was recorded by the microscope. In figure 3.3 the needle gradually moved towards the left (x direction). Note that the needle also moved a little out of focus. The positioning of the needle was done

manually and prevented perfect alignment of the needle in the x-plane. Due to this imperfect positioning the needle also bended slightly in the y-direction, explaining the F_y as seen in the graph. The time series also clearly show the lack of the gel 'rupturing' near the tip of the needle. This could be due to the material properties, but could also mean that the magnification is too low: the rupture might simply be too small to observe with a 20x magnification. In figure 3.4 the images of the gel where the needle was inserted clearly show the gel closing after the needle up to a certain point.

4.2 Relating Graphs to Images

The images taken with the microscope and the graphs recorded by LabView are hard to relate to each other. The microscope scans an image over a time of 2 s, which means that different parts of the image belong to different recorded forces. Besides that, there is no absolute measure for which range of forces belong to which image. On the recorded images we can see when the needle enters the gel, but that is still in a range of 2 s and the exact insertion moment can not clearly be seen in the graphs because the force of the initial contact can not be distinguished from the no needle-gel contact situation. Still we can qualitatively discuss on the results because the different phenomena that were recorded, generally occur over a time longer than two seconds.

4.3 Shearing

During a few of our experiments the gel sheared from the sample glass. This phenomenon was also recorded by the microscope, as can be seen in figure 3.23. The arrow in this image points to the moment where the shearing stops and normal insertion continues. Shearing apparently lowered the force required to insert the needle, while it increased the torque. We suspect shearing most likely to occur when the needle is positioned too close to the glass.

4.4 Dark lines

In some of the images there are dark lines in the gel. The dark lines at the edge are due to the ragged edges left by cutting the gel. However due to the mold in which the gel was made, which was available at the lab, the gel also had several circular protrusions. The edges of these protrusions resulted in dark lines on the images recorded by the microscope. To prevent this, either the needle will have to be positioned more carefully so that its path does not go over the protrusions, or another mold without the circular extrusions will have to be used. An example of these dark lines in the images can be found in figure 3.18, where both the edge of the gel and a protrusion can be seen.

4.5 Needle bending

As already discussed in Section 4.1, the needle bended during insertion by asymmetrical forces acting on the needle[6]. After the movement was stopped and the system relaxed, the needle slowly bended back toward its neutral position.

This effect can be observed on the last image of figure 3.6. The arrow points to where a line in the gel shows the position of the needle before relaxation. At a certain point, when the needle has pushed enough gel away, air will enter the insertion shaft and interferes with our ability to image the needle clearly: as the microscope can not distinguish between air and needle, it is all shown as black and we lose our view of the needle.

The relaxation of the needle might also change the shape of the shaft after needle retraction, depending on how long the system has had time to reach an equilibrium.

4.6 Microneedles

The microneedles were tested in the same way as the rest, but showed no bending. The silicon base makes them rigid and explains why no bending was observed, while torques were recorded during the experiments. There was something strange going on with the imaging: on the third time of figure 3.9 the tip and a 'shadow' of the tip were recorded. This indicates that the tip suddenly displaced during the scan. Since this was not observed with other needles, it may be an effect caused by the stiff microneedles. Further research will be needed to confirm this. One can also observe some sort of 'turbulence' in the transmitted light images, but this does not seem to have any effect on the fluorophore density.

Taking a closer look at figure 3.8, one can see that F_z did not increase after about 1 mm displacement. This is about the size of the tip: after 1 mm the frontal area in the gel was constant.

4.7 Higher insertion speeds

The force and torque measurements of the experiments that were run at 0.5 mm/s and 1 mm/s also produced higher forces and torques with respect to the 0.1 mm/s ones. Unfortunately the microscope scans quite slowly and thus the images per experiment also decrease at higher insertion speeds. Explaining anomalies in the force and torque readings can become hard without corresponding images. Especially the 1 mm/s measurements have very few images. This is a very large disadvantage, also because the image is scanned over a time of 2 s. This means that each line of the image is of a later time than the previous one; in fact every pixel differs a bit from the previous one. The resulting image is not a snapshot, but a collection of different pixels at different times, which can make the image look warped. This warping can be seen in figure 3.18, where it seems as if the needle is inserted at a different angle, while actually the needle has moved so much between two scan lines that it only looks this way.

There is also a decreasing force as the needle stops at its end position. This can be explained with the controller which is programmed to stop at a specific position and starts decelerating before reaching it.

5 Conclusion

We were able to construct the set-up as required: we can observe needle-tissue interactions under the LSM and measure the forces involved in this interaction. The results are reproducible and anomalies can be explained. Though we are not (yet) able to observe rupturing of the gel, there are some very interesting phenomena taking place: the bending of the needle as well as the relaxation after insertion, turbulence at the straight edge of microneedles, closing of the gel after retraction and the shearing. These effects might give us more insight into needle-tissue interactions.

6 Recommendations

To improve the set-up, a way to align the needle more accurately might reduce the needle bending out of focus. Faster imaging will improve the images and provide clearer images at higher insertion speeds. Exploring the bi-directional scanning functionality of the microscope

might prove useful. Using a higher magnification in combination with the microneedles might show the rupturing of the gel at small scale, because the microneedles do not bend as much as the hypodermic needles. Using more human-like material that can simulate needle-cell interaction as specimen could provide more insight into what happens around the needle. Especially if we could be able to observe cells closing the penetration shaft after retracting the needle would be a very interesting research topic.

7 Acknowledgments

I would like to thank Gerben te Riet o/g Scholten for all the assistance with orders, construction and configuration of the set-up; Rob Reilink for the mechanical advice and Alfred de Vries for the LabView instructions. From the Nanobiophysics group I would like to thank Tom Groothuis for all the instructions and help with using the confocal microscope as well as Vinod Subramaniam for allowing us to use the confocal microscope.

References

- [1] S. Misra, K. Reed, K. Ramesh, and A. Okamura, "Observations of needle-tissue interactions," in *Proceedings of the 31st Annual International Conference of the IEEE Engineering in Medicine and Biology Society: Engineering the Future of Biomedicine, EMBC 2009*, pp. 262–265, 2009.
- [2] P. Walln, K. Carlsson, A. Liljeborg, and S. Grillner, "Three-dimensional reconstruction of neurons in the lamprey spinal cord in whole-mount, using a confocal laser scanning microscope," *Journal of Neuroscience Methods*, vol. 24, no. 2, pp. 91 – 100, 1988.
- [3] K. Koren, "FITC." http://www.fluorophores.tugraz.at/Show_SearchResult.php?Substance_ID=252, Visited: Januari 2011. Graz University of Technology Institute for Analytical Chemistry.
- [4] W. Chan, "Instrumentation to characterize needle insertion into biological tissue," Master's thesis, Massachusetts Institute of Technology, 2002.
- [5] W. Ahn, J.-H. Bahk, and Y.-J. Lim, "The Gauge System for the Medical Use," *Anesthesia & Analgesia*, vol. 95, no. 4, p. 1125, 2002.
- [6] S. Misra, K. Reed, A. Douglas, K. Ramesh, and A. Okamura, "Needle-tissue interaction forces for bevel-tip steerable needles," in *Proceedings of the 2nd Biennial IEEE/RAS-EMBS International Conference on Biomedical Robotics and Biomechatronics, BioRob 2008*, pp. 224–231, 2008.

8 Scientific Output

Using the device described in this report, the following scientific publications were created:

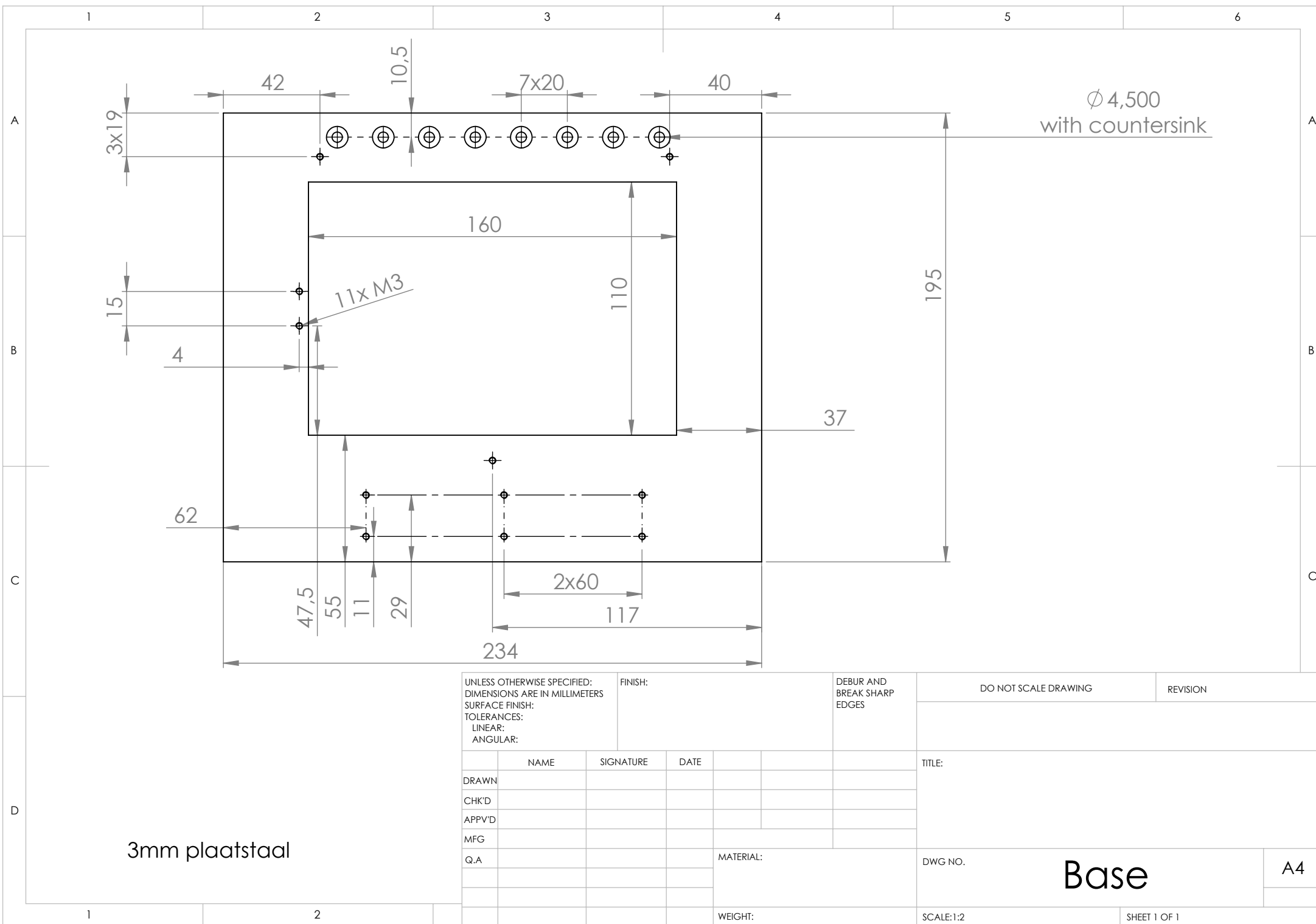
1. A. Jahya and S. Misra, "Microscopic observations of needle and soft-tissue simulant interactions" in *International Society of Biomechanics Congress, Brussels, Belgium*, July 2011. (Under review)
2. P. Trapper, A. Jahya, S. Misra, and K. Bertoldi, "Fracture Mechanics-Based Models of Needle-Tissue Interactions". (In Preparation)
3. G. Krishnamoorthy, A. Been, S. Misra and N. Tas, "In-situ Observations of Gel-Rupture by Microneedles : An Integrated set-up for Real-time Imaging Using Confocal Microscopy and Needle Penetration Force Measurements". (In Preparation)

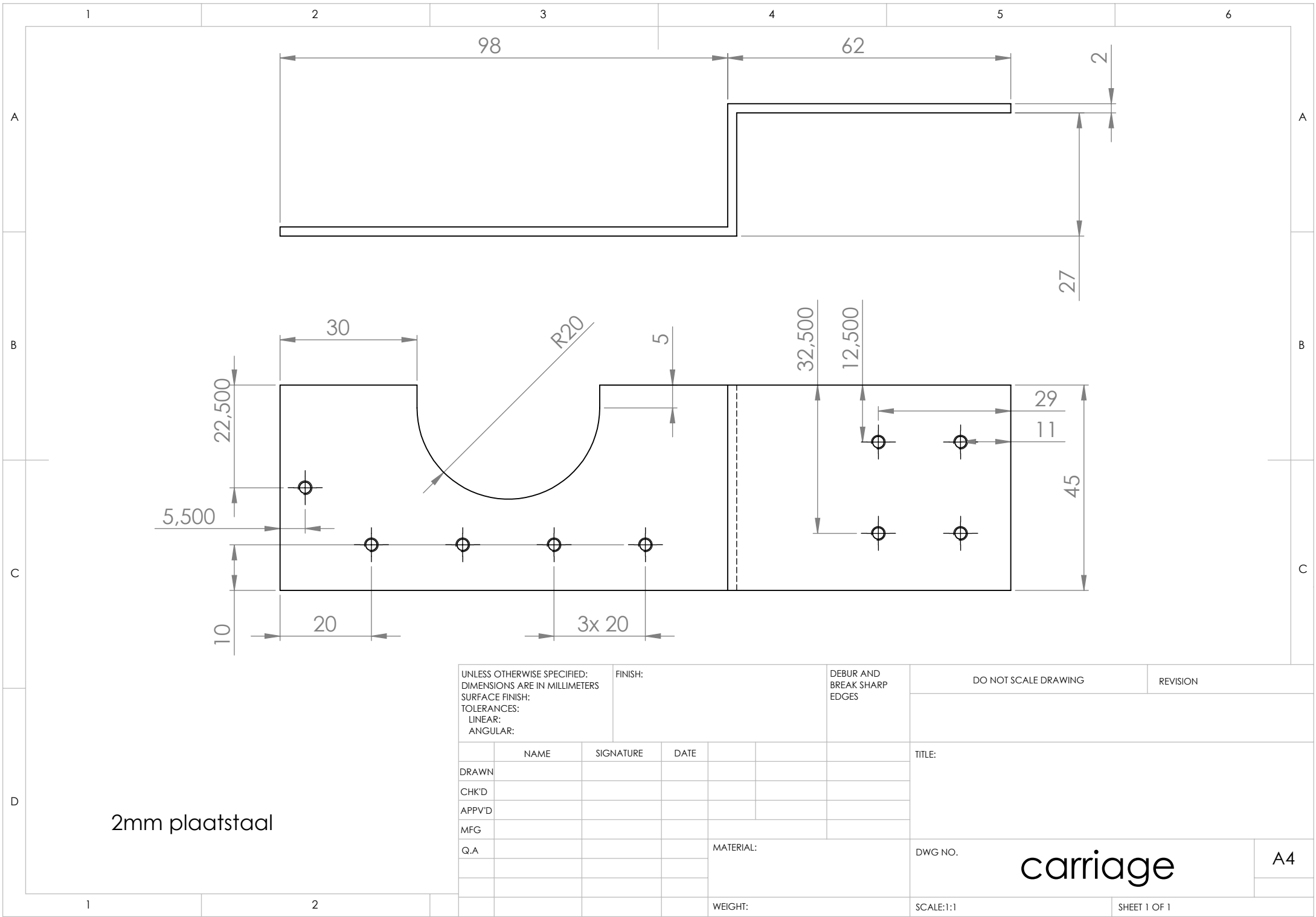
Appendices

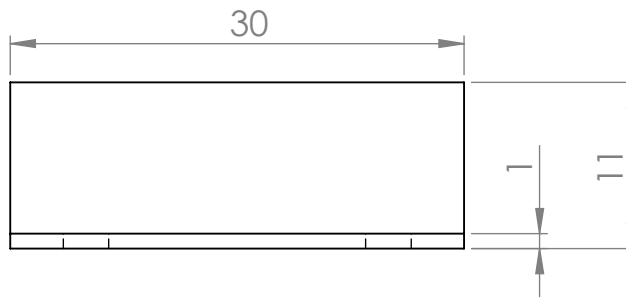
A Mechanical Drawings

The drawings of the design are included on the following pages. The prefabricated parts are:

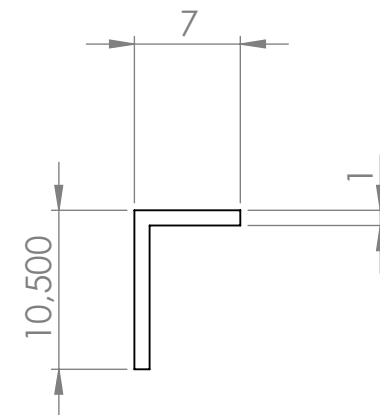
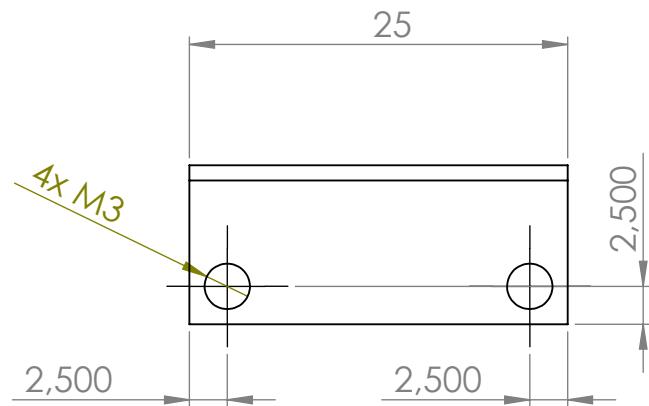
- From MiSUMi (<http://www.misumi-europe.com>)
 - Single Axis Actuators LX20 Standard Type LX2001-B1-A2025-150
 - Dovetail X-Axis Stages Hexagon Wrench Type XEEG25
 - Miniature Slide Guides Short/Preload Advanced Class Selectable Type SEBS10-155-MC
 - Couplings Single Disc High Torque Set Screw Type MCKS10-4-4
 - Magnet with Holder Thin Type (6 mm, 1018 steel eq., nickel plating, cobalt magnet) HXM6
 - Magnets Square Round Type (D 5mm, L 3mm, cobalt magnet) HXMS5-3
- From Maxon (<http://www.maxonmotor.nl/>) Combination number: 304547
 - 283858 EC-max22 25W 24V
 - 143974 GP22C 14:1
 - 201940 MR type M 512imp/rev.
- From ATI (<http://www.ati-ia.com>)
 - 9105-TW-NANO17-E-1.8 NANO17-E Transducer with Strain Relieved Cable, 1.8m
 - 9105-IFPS-1 Interface board and power supply for (1) F/T transducer
- From Farnell (<http://nl.farnell.com/>)
 - 1518997 CHERRY - DB2C-A1LC - MICROSWITCH, SPDT, MED LEVER
 - 1082379 APEM - A01ES+A0154B - EMERGENCY SWITCH, DPDT
 - 1701582 BULGIN - BEP03SBB0 - ENCLOSURE, BLACK, 80X139MM, IP67
 - 9793550 SCHURTER - 1241.2801 - PUSHBUTTON SWITCH
- From Elmo (<http://www.elmomc.com/>)
 - Whistle 2.5A motor controller



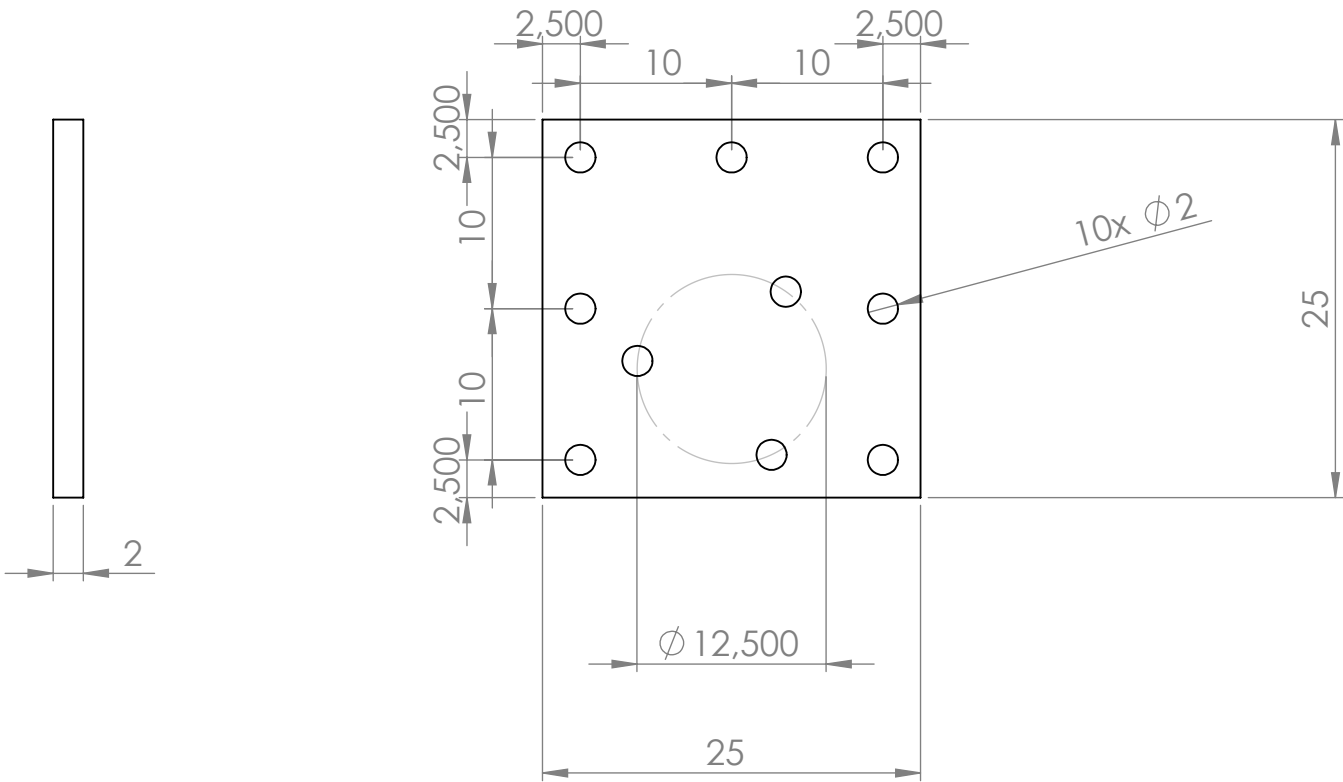




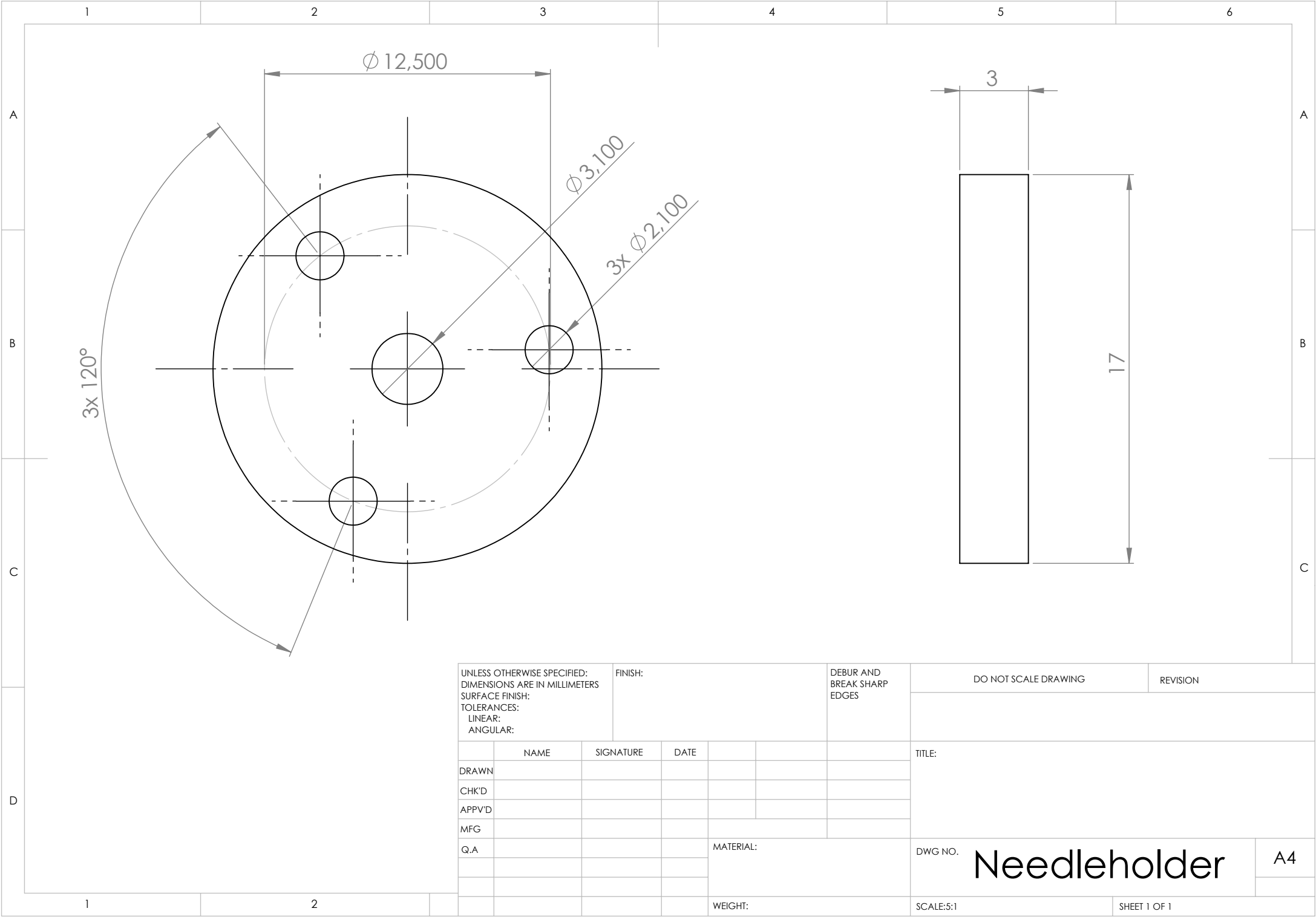
1mm aluminium



DWG NO. adj stage mount.v2^{A4}



UNLESS OTHERWISE SPECIFIED: DIMENSIONS ARE IN MILLIMETERS SURFACE FINISH: TOLERANCES: LINEAR: ANGULAR:				FINISH:			DEBUR AND BREAK SHARP EDGES		DO NOT SCALE DRAWING		REVISION		
	NAME	SIGNATURE	DATE				TITLE:						
DRAWN													
CHK'D													
APPV'D													
MFG													
Q.A				MATERIAL:			DWG NO.		sensorholder			A4	
				WEIGHT:			SCALE:2:1		SHEET 1 OF 1				



B Results

The following pages show all the force and torque graphs of the experiments.

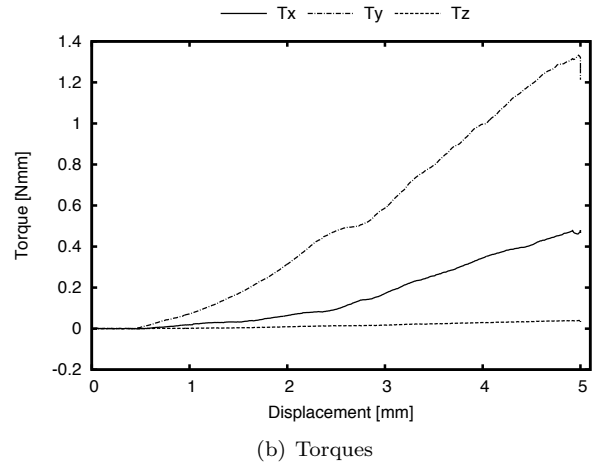
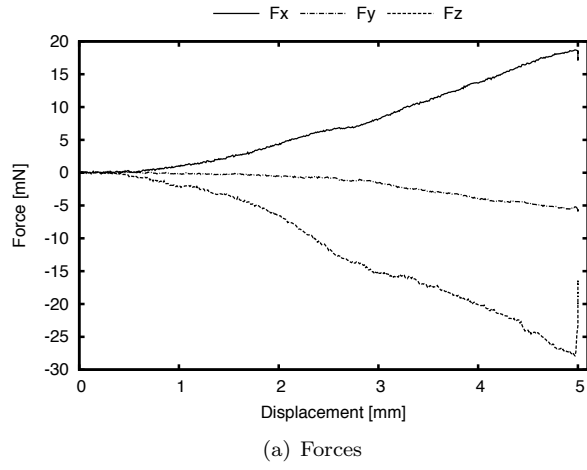


Figure B.1: 0.1 mm/s 19G - 1

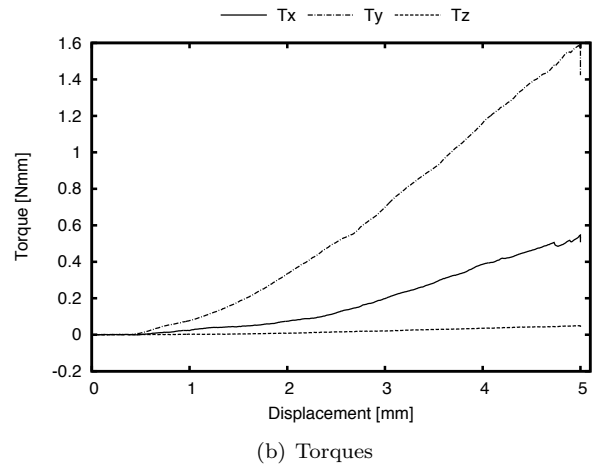
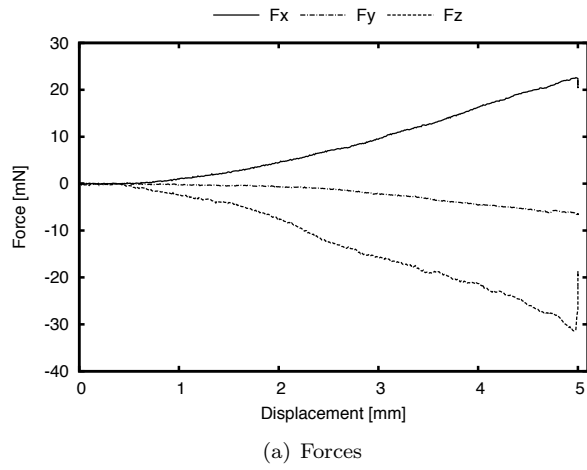


Figure B.2: 0.1 mm/s 19G - 2

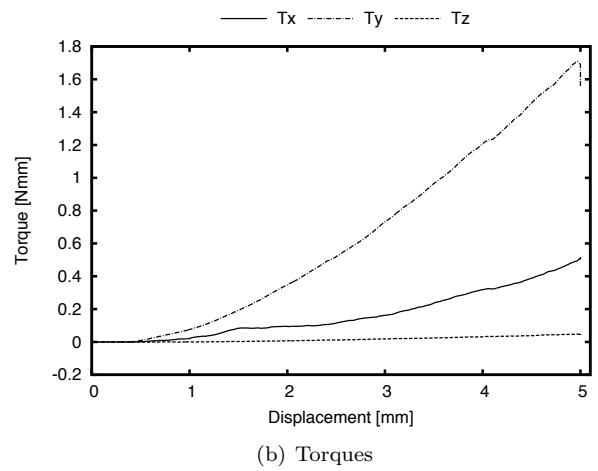
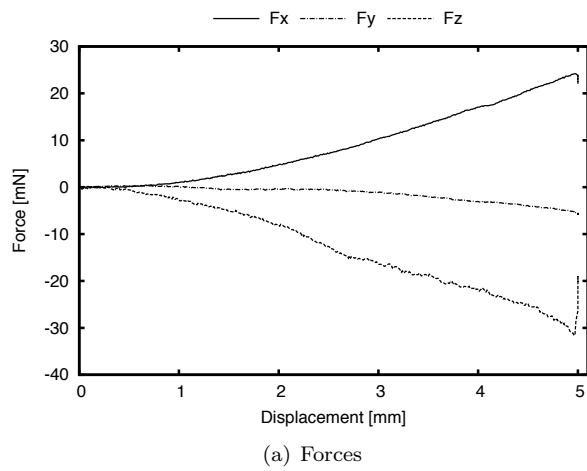
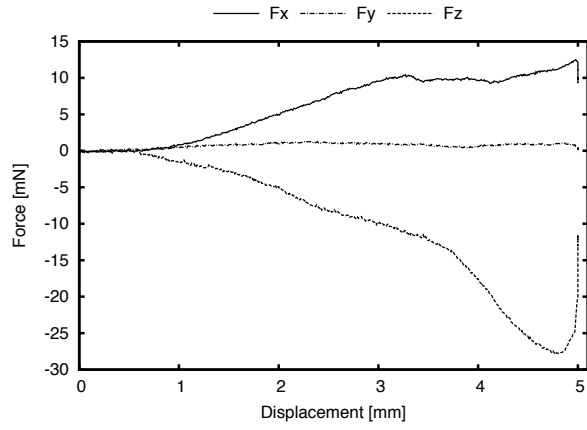
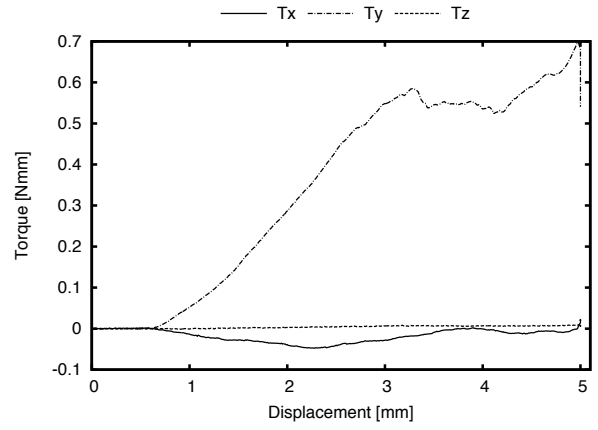


Figure B.3: 0.1 mm/s 19G - 3

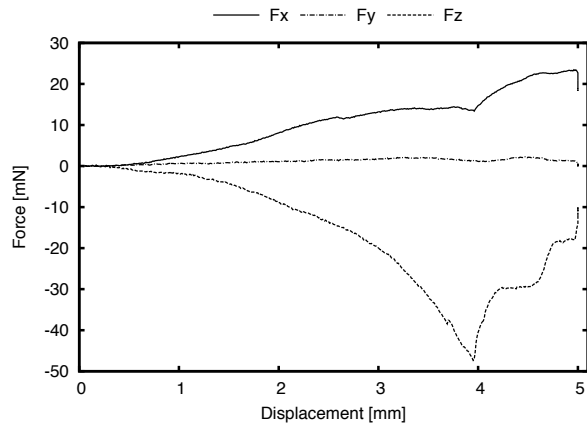


(a) Forces

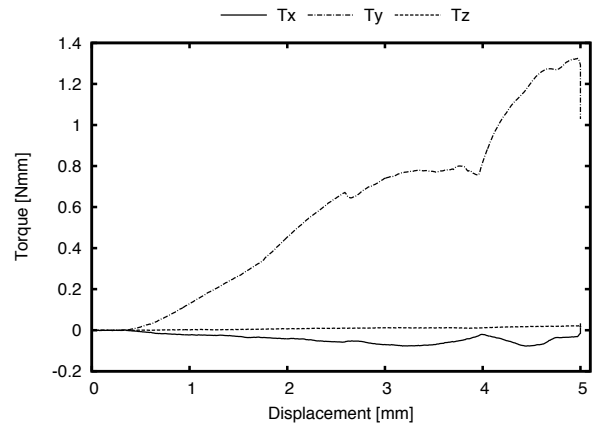


(b) Torques

Figure B.4: 0.1 mm/s 21G - 1

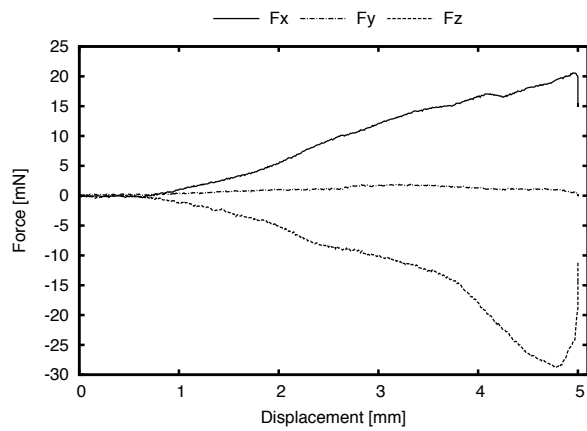


(a) Forces

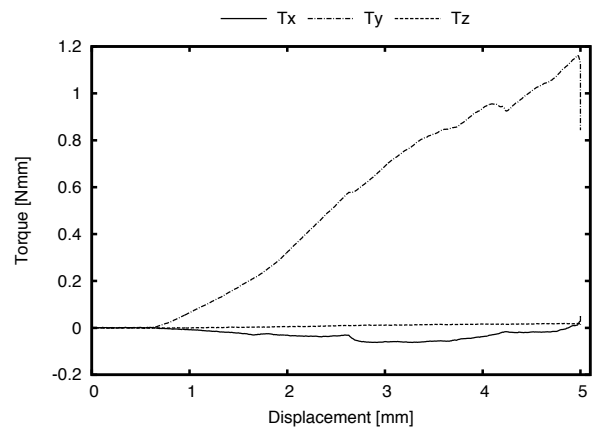


(b) Torques

Figure B.5: 0.1 mm/s 21G - 2



(a) Forces



(b) Torques

Figure B.6: 0.1 mm/s 21G - 3

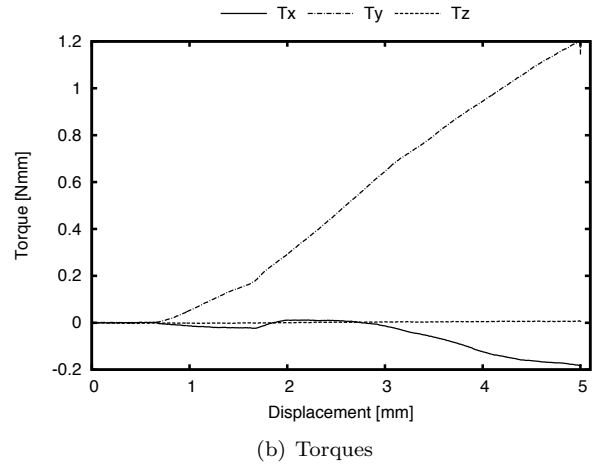
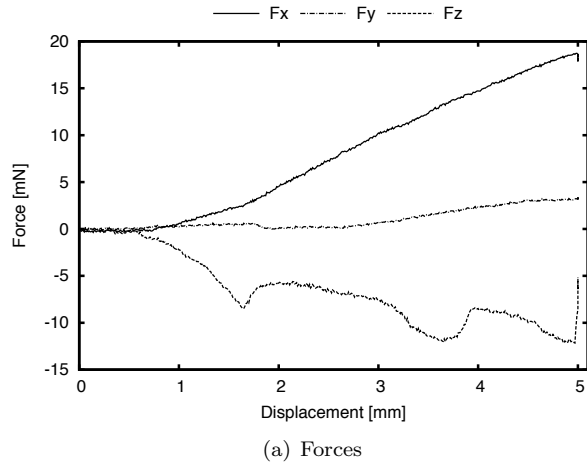


Figure B.7: 0.1 mm/s 23G - 1

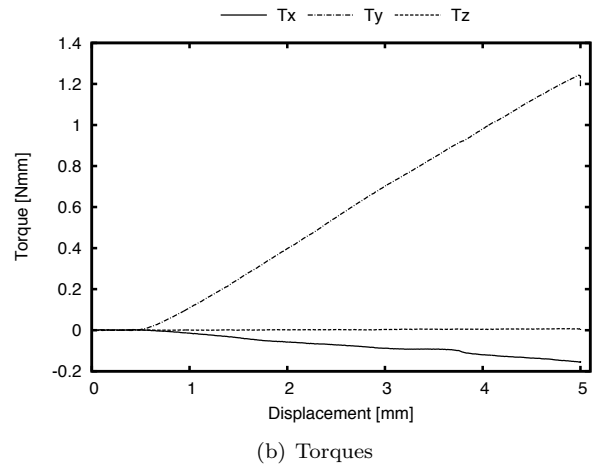
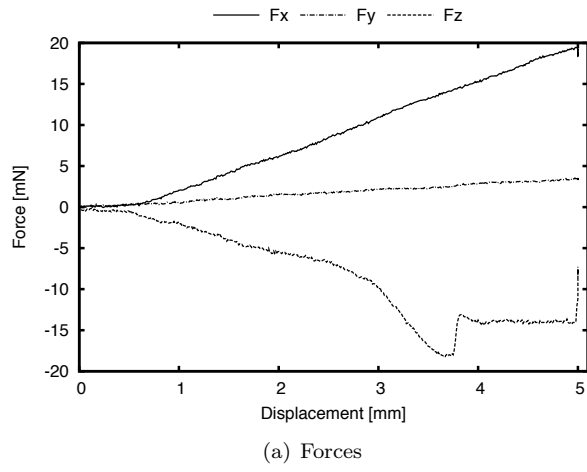


Figure B.8: 0.1 mm/s 23G - 2

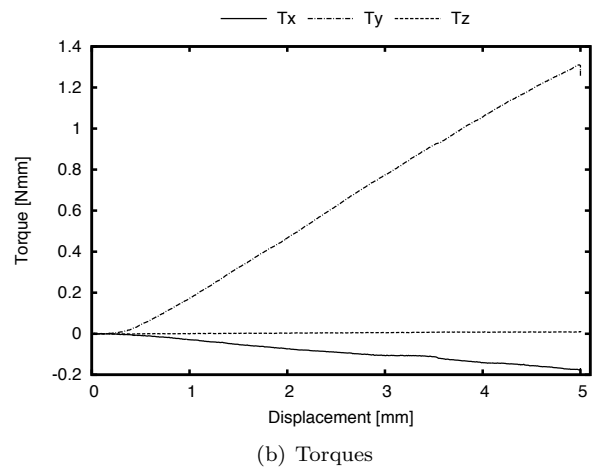
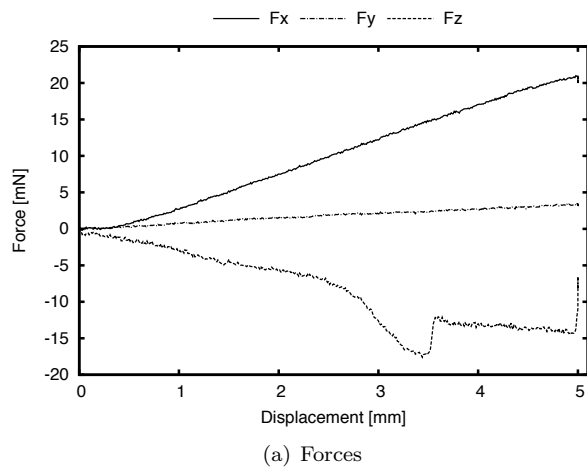


Figure B.9: 0.1 mm/s 23G - 3

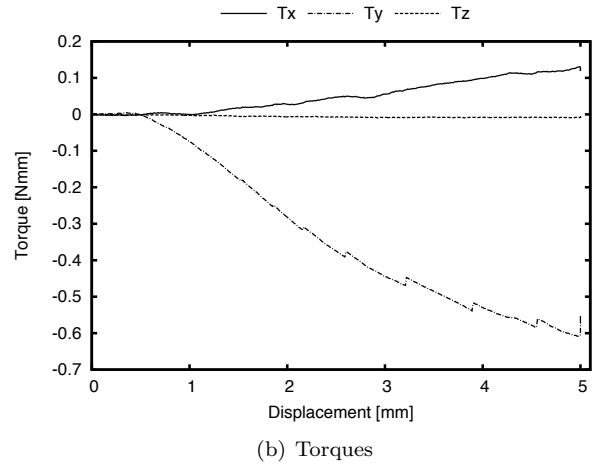
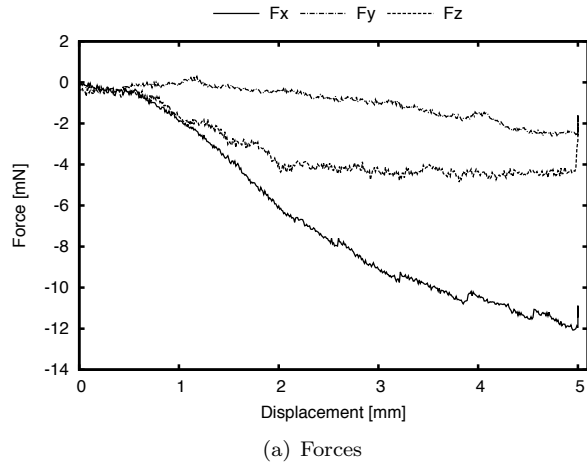


Figure B.10: 0.1 mm/s 27G - 1

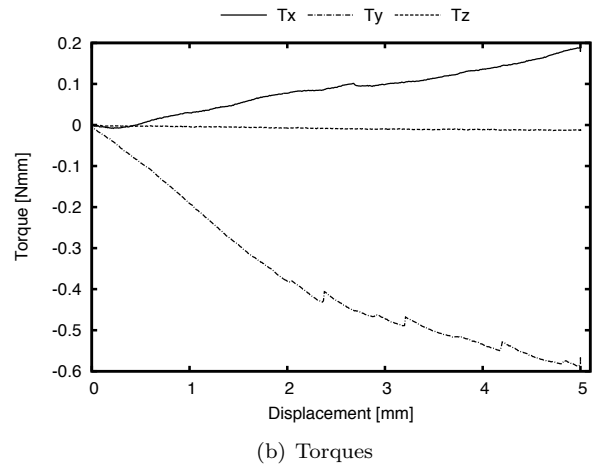
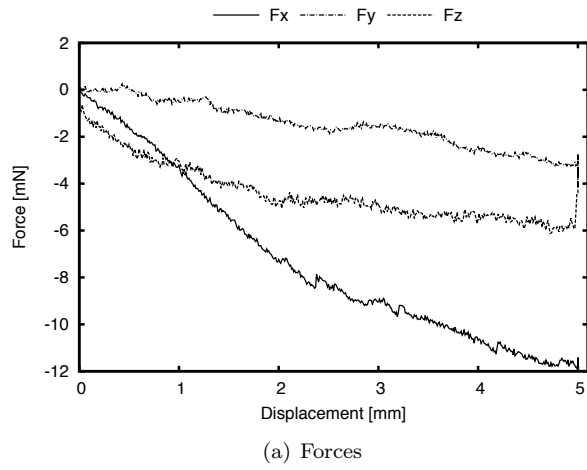


Figure B.11: 0.1 mm/s 27G - 2

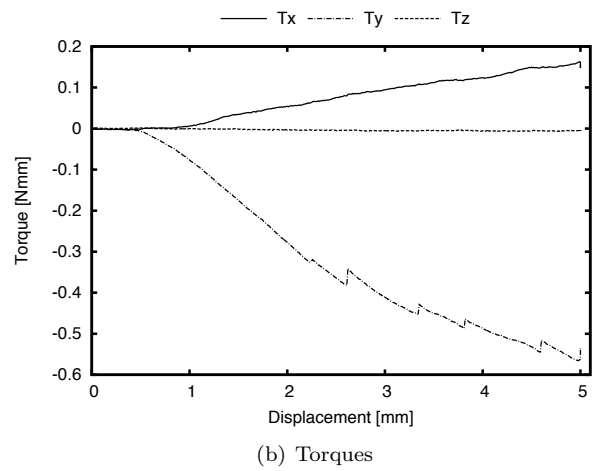
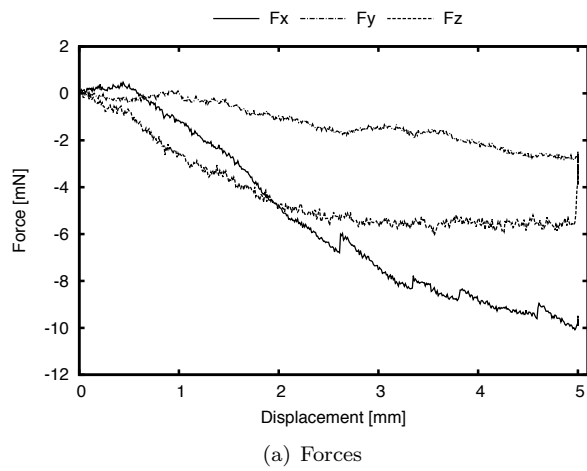


Figure B.12: 0.1 mm/s 27G - 3

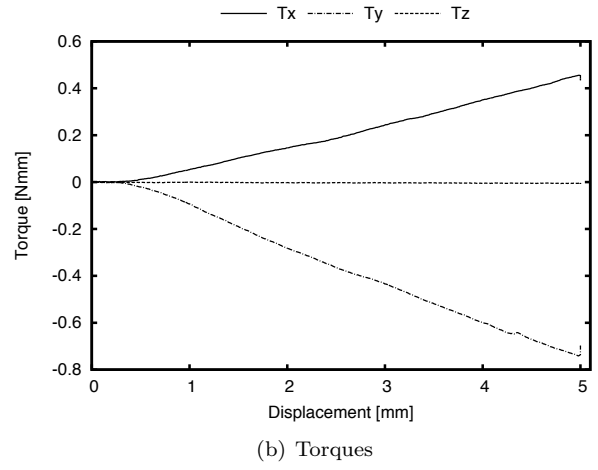
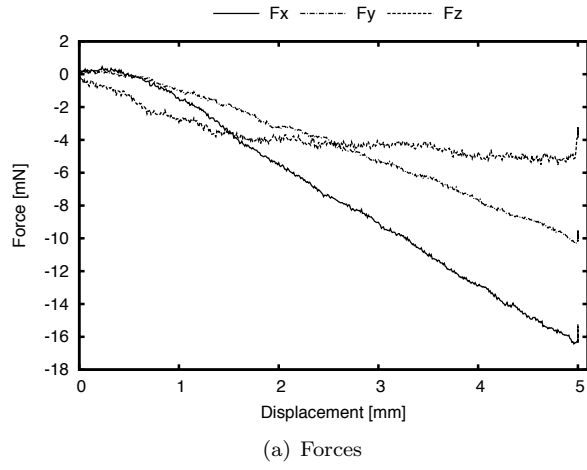


Figure B.13: 0.1 mm/s 30G - 1

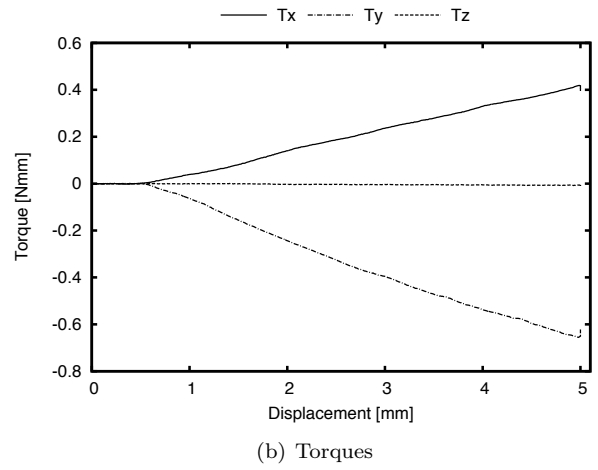
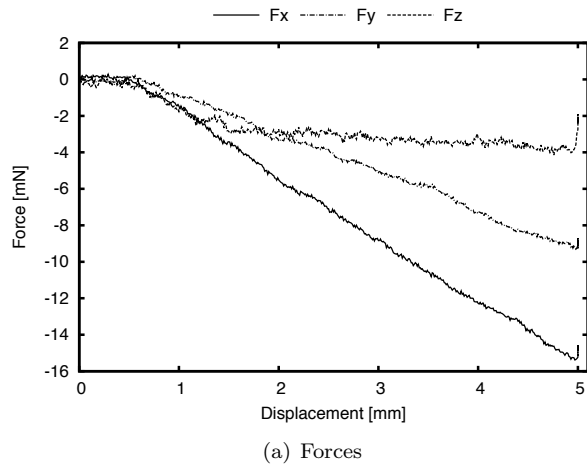


Figure B.14: 0.1 mm/s 30G - 3

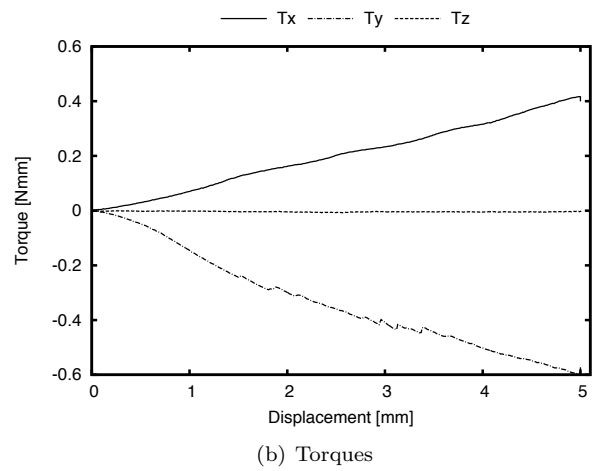
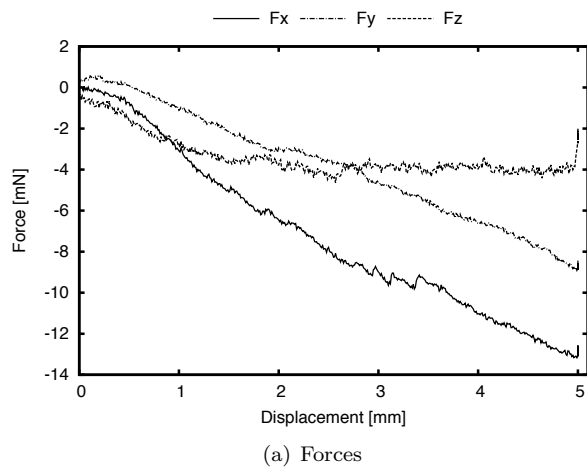
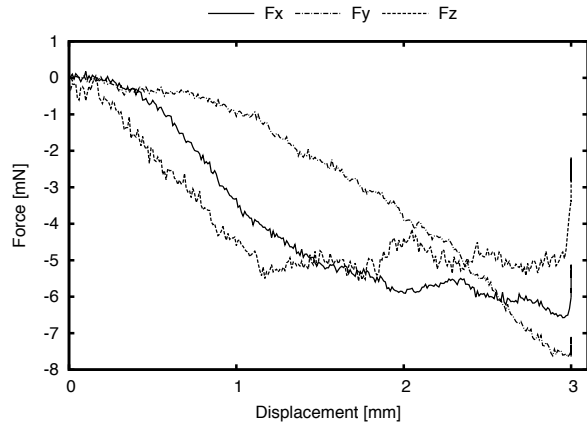
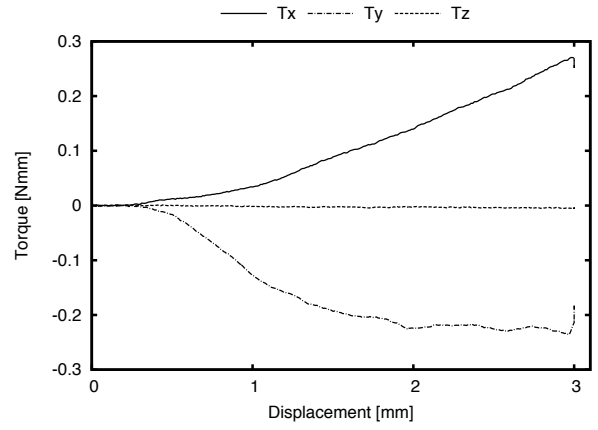


Figure B.15: 0.1 mm/s 30G - 4

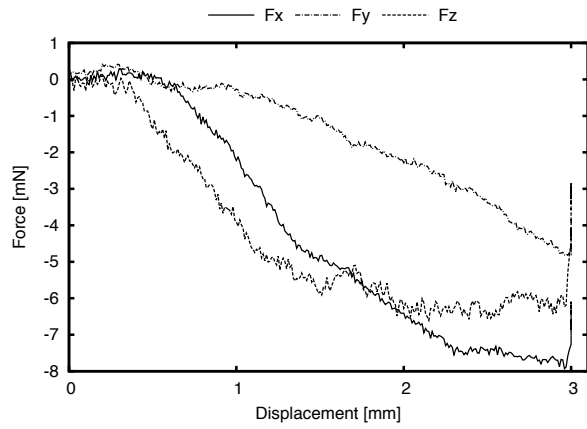


(a) Forces

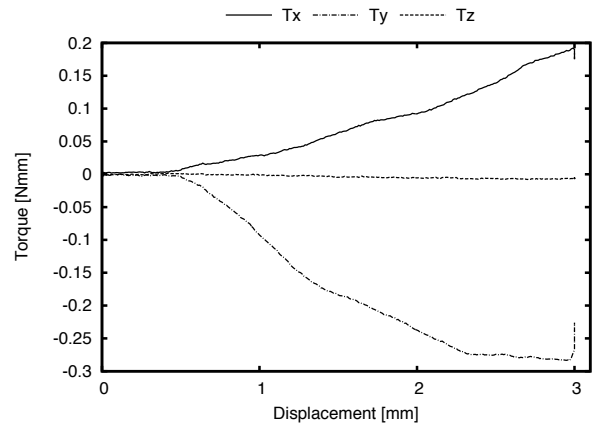


(b) Torques

Figure B.16: 0.1 mm/s *penelope* 200×400 - 1

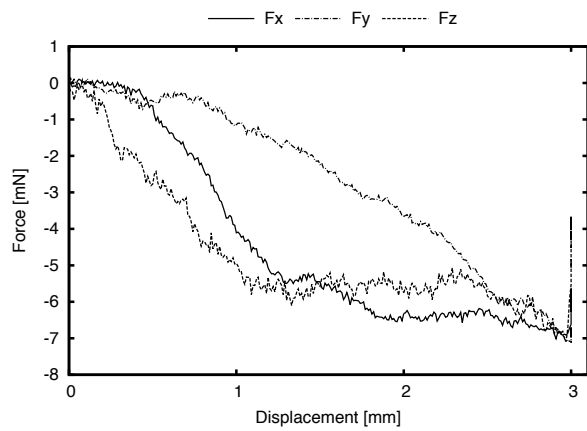


(a) Forces

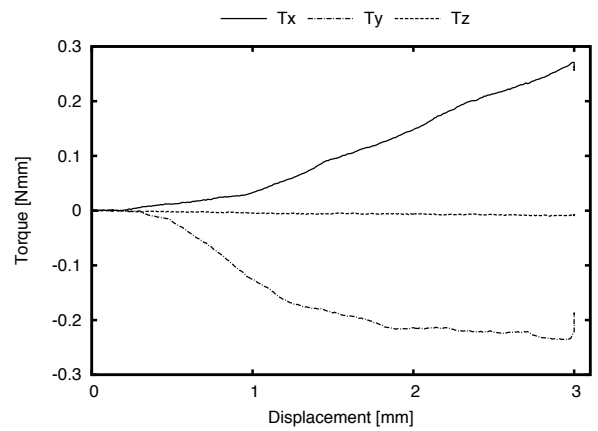


(b) Torques

Figure B.17: 0.1 mm/s *penelope* 200×400 - 2



(a) Forces



(b) Torques

Figure B.18: 0.1 mm/s *penelope* 200×400 - 3

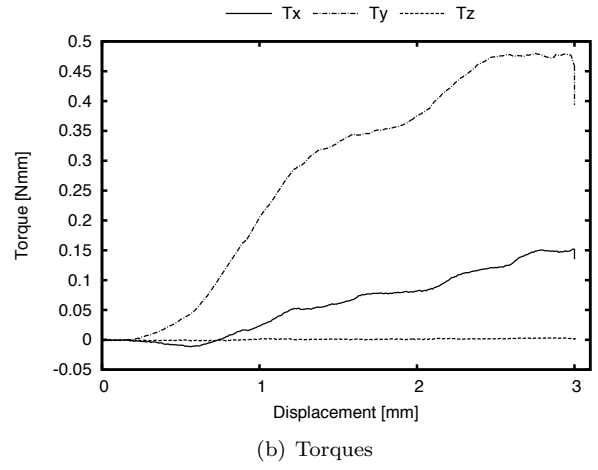
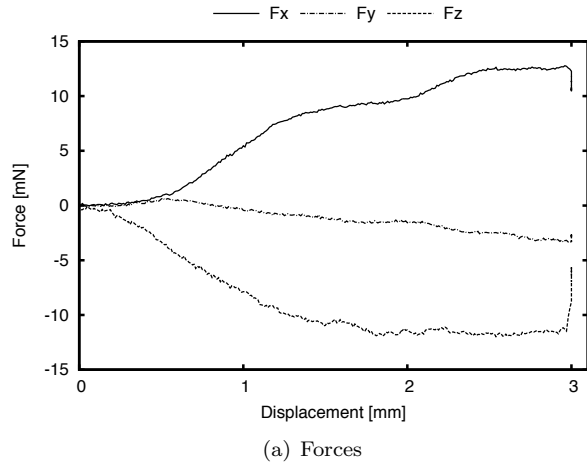


Figure B.19: 0.1 mm/s *penelope* 400×400 - 1

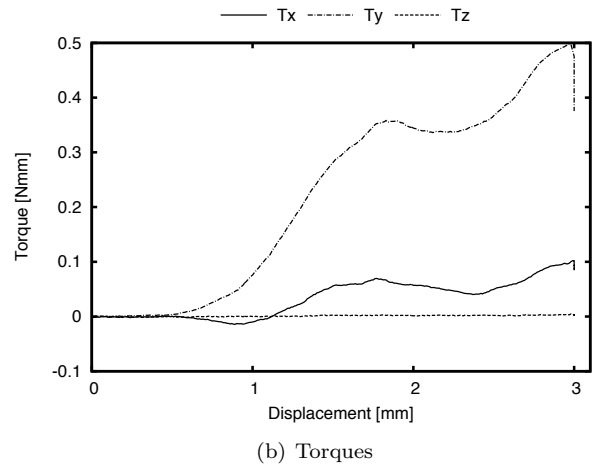
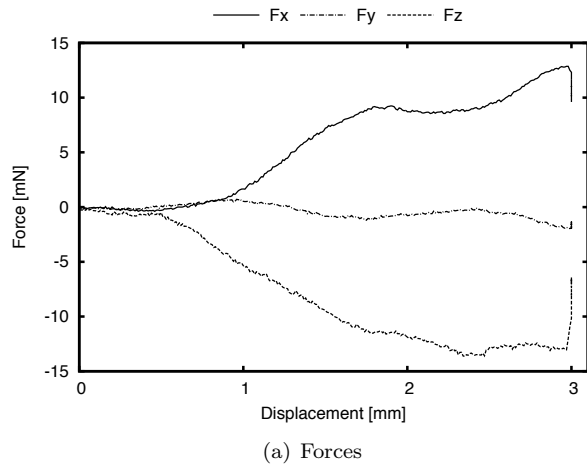


Figure B.20: 0.1 mm/s *penelope* 400×400 - 2

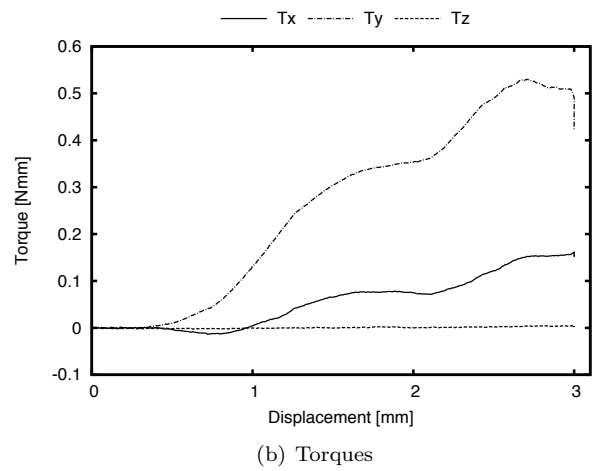
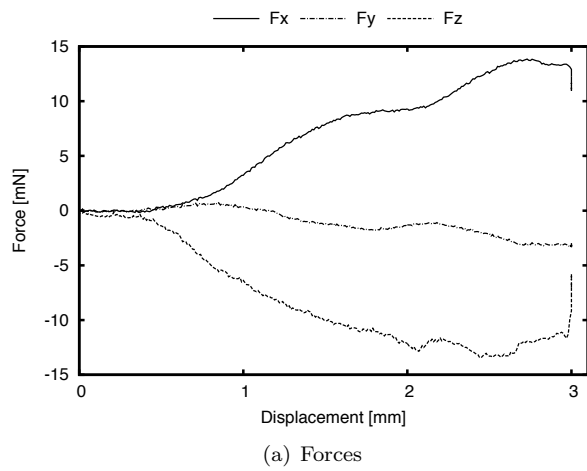
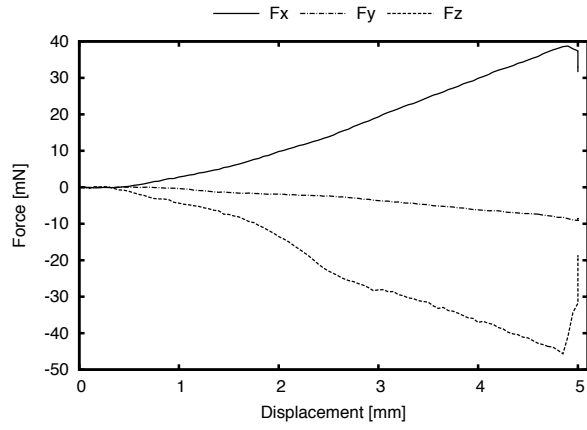
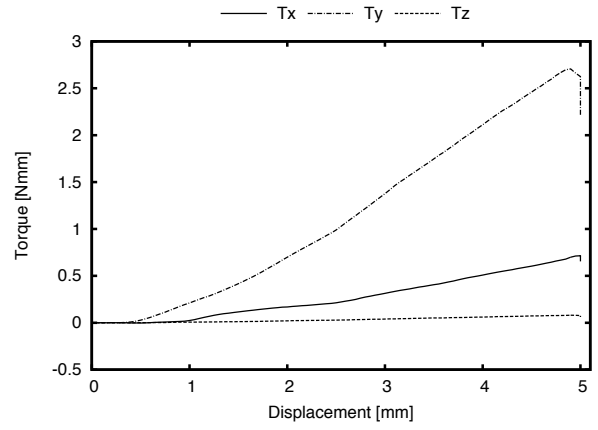


Figure B.21: 0.1 mm/s *penelope* 400×400 - 3

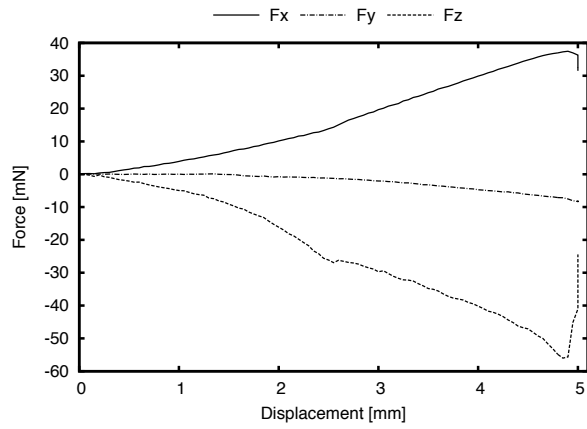


(a) Forces

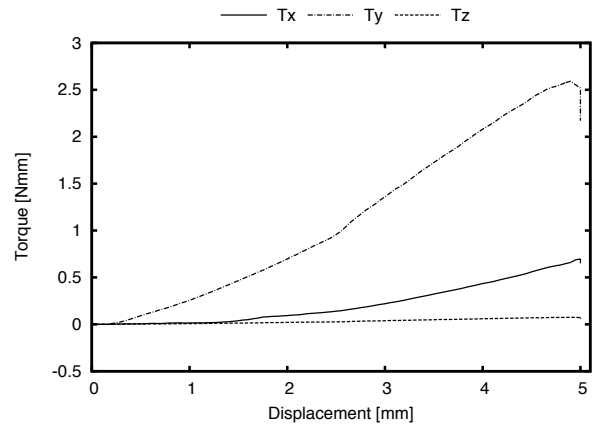


(b) Torques

Figure B.22: 0.5 mm/s 19G - 1

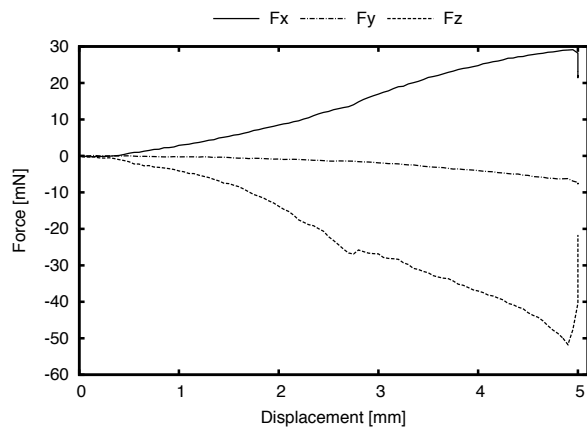


(a) Forces

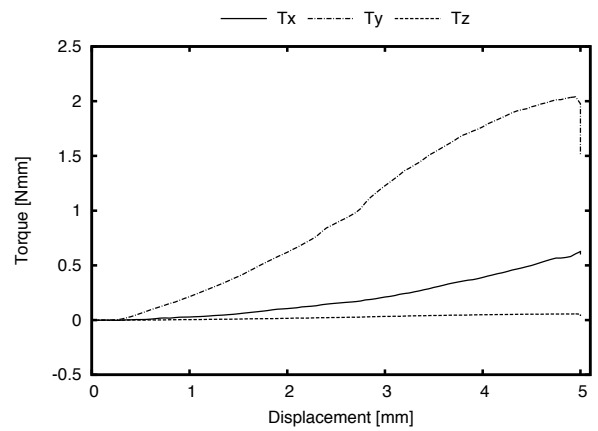


(b) Torques

Figure B.23: 0.5 mm/s 19G - 2

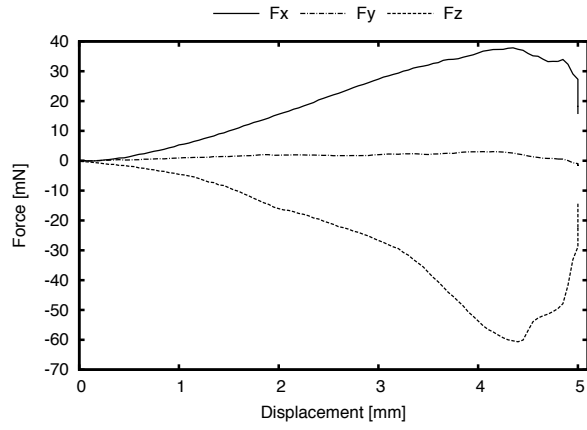


(a) Forces

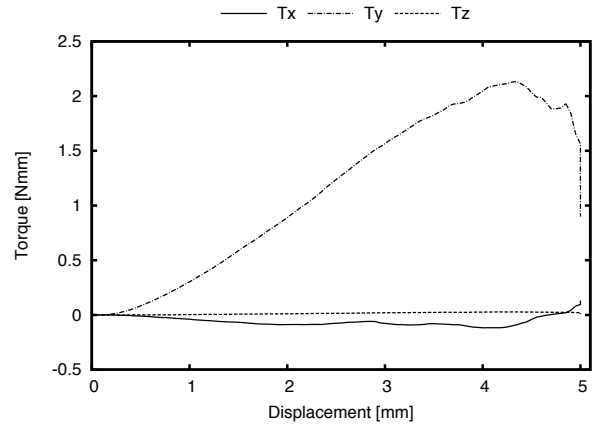


(b) Torques

Figure B.24: 0.5 mm/s 19G - 3

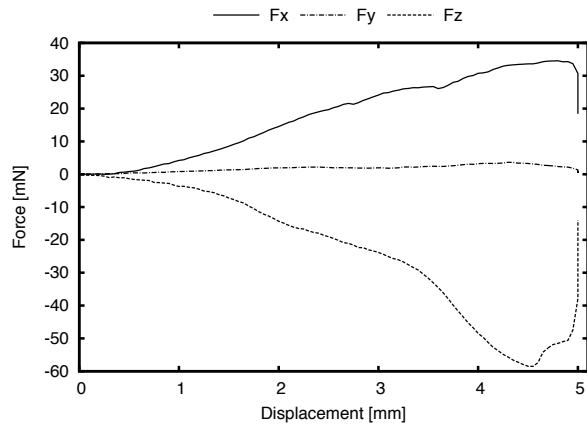


(a) Forces

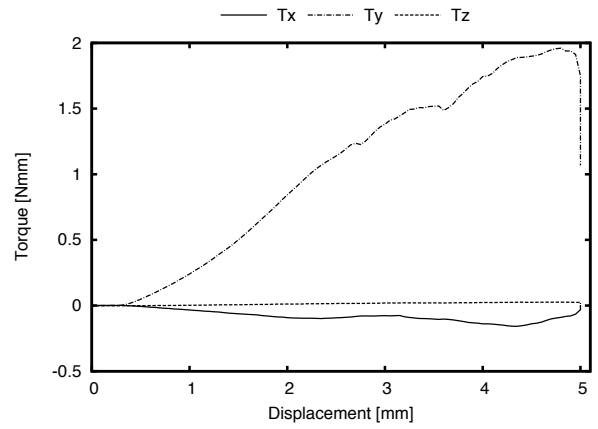


(b) Torques

Figure B.25: 0.5 mm/s 21G - 1

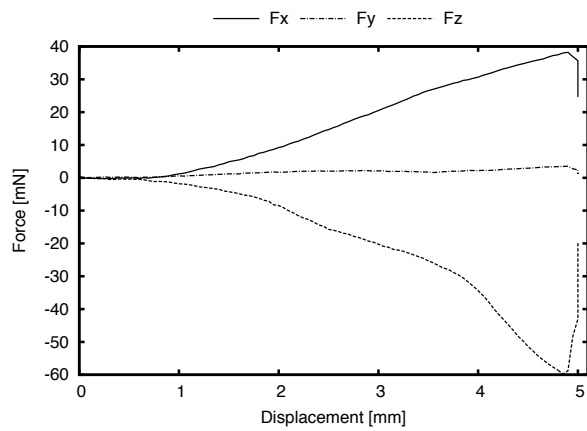


(a) Forces

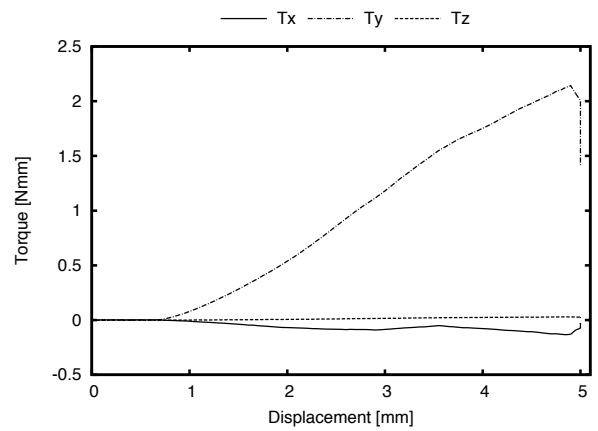


(b) Torques

Figure B.26: 0.5 mm/s 21G - 2



(a) Forces



(b) Torques

Figure B.27: 0.5 mm/s 21G - 3

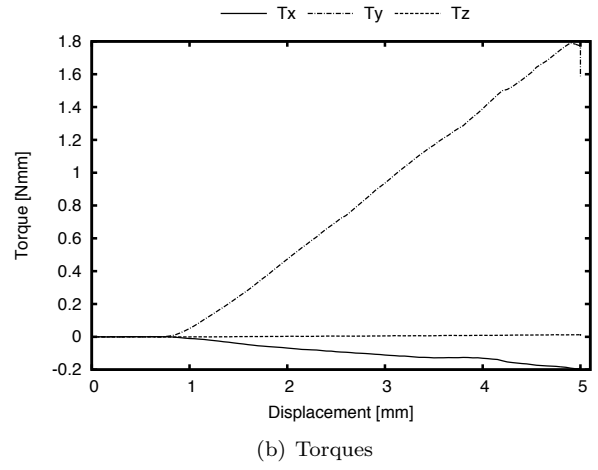
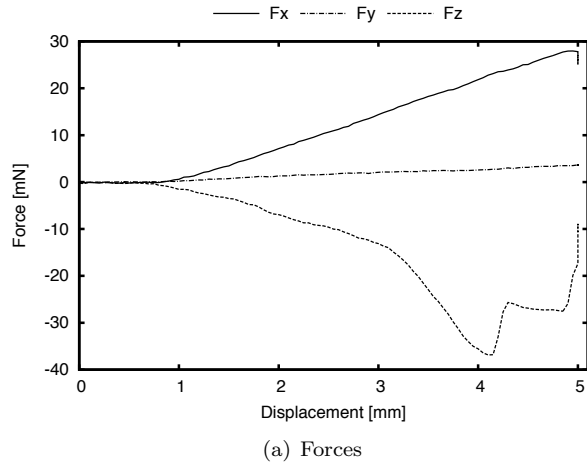


Figure B.28: 0.5 mm/s 23G - 2

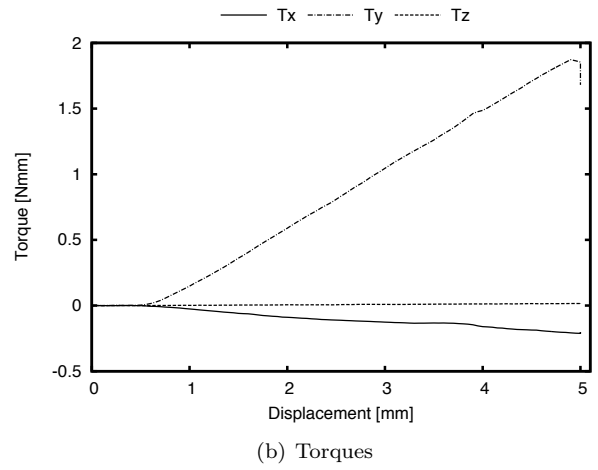
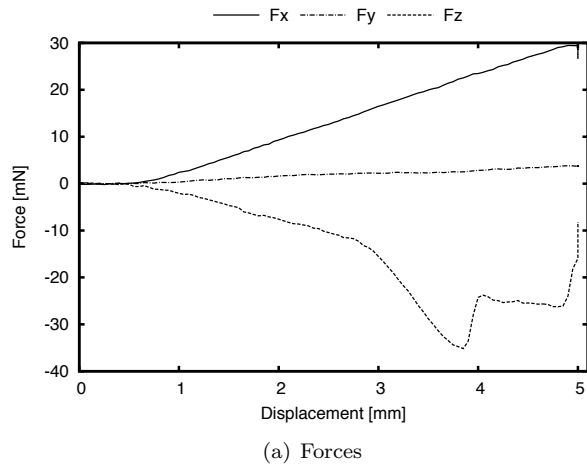


Figure B.29: 0.5 mm/s 23G - 3

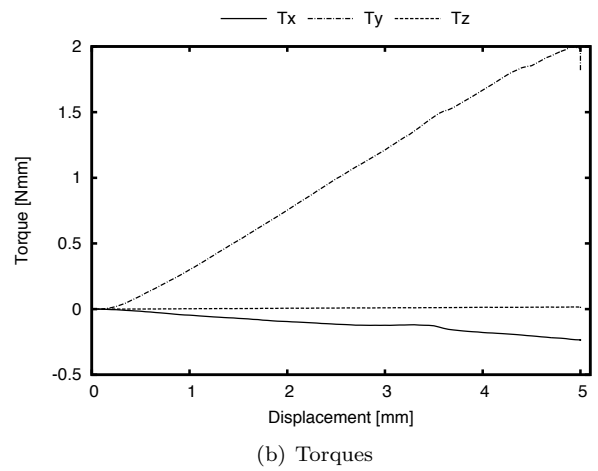
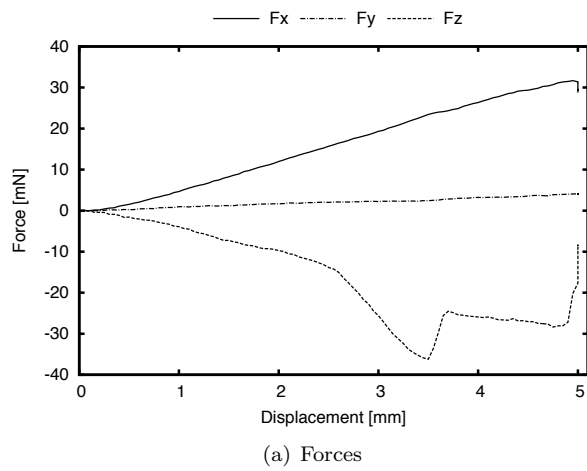


Figure B.30: 0.5 mm/s 23G - 5

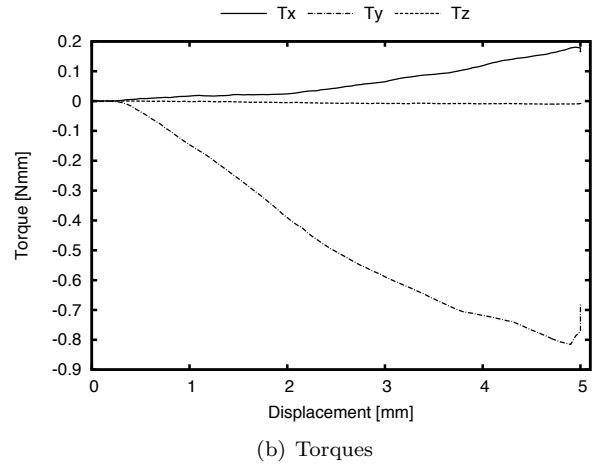
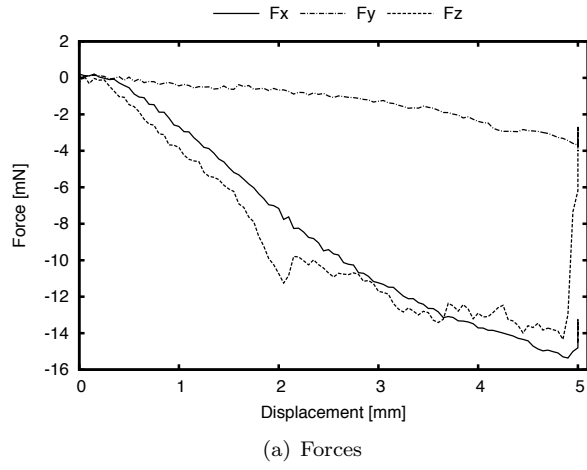


Figure B.31: 0.5 mm/s 27G - 1

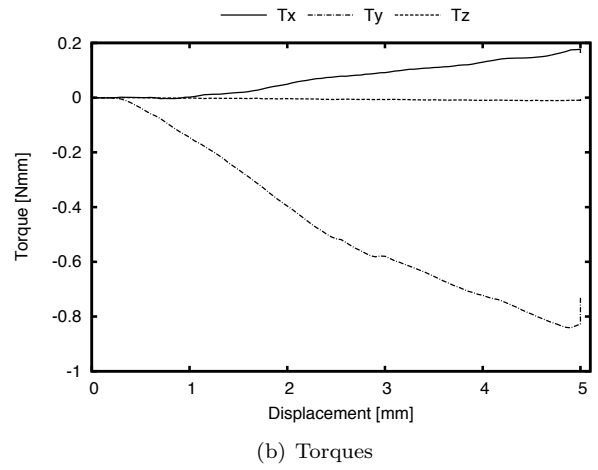
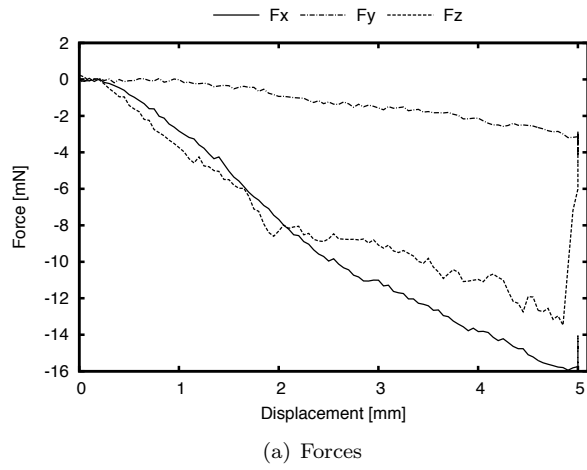


Figure B.32: 0.5 mm/s 27G - 2

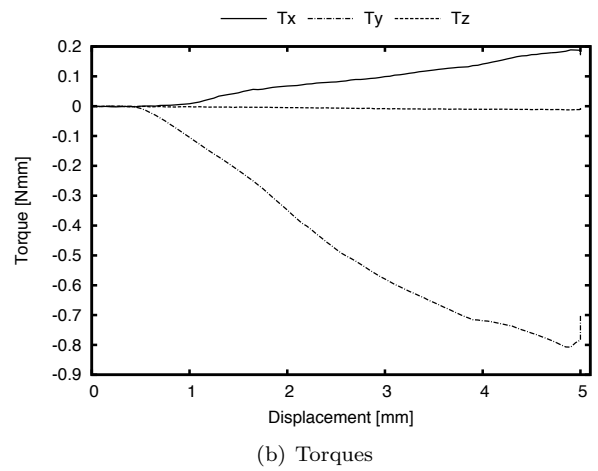
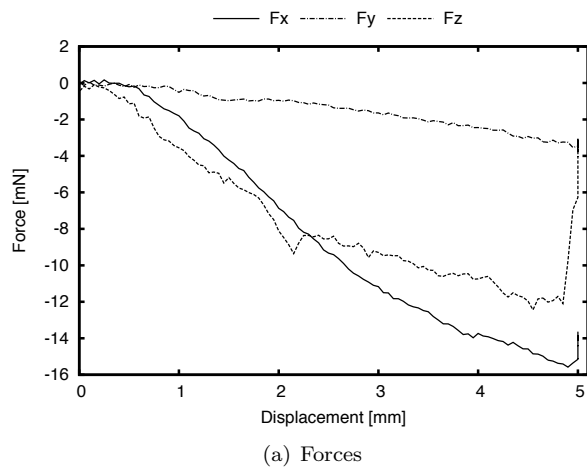
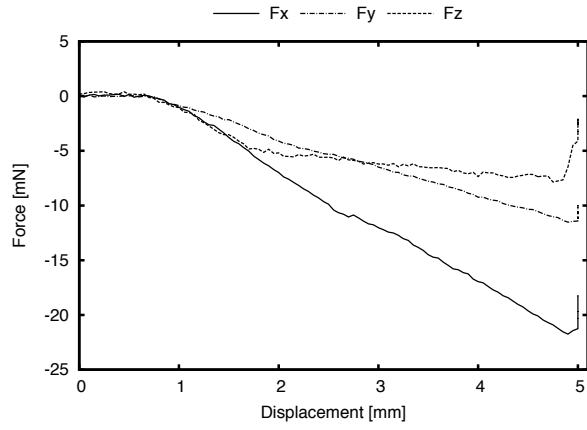
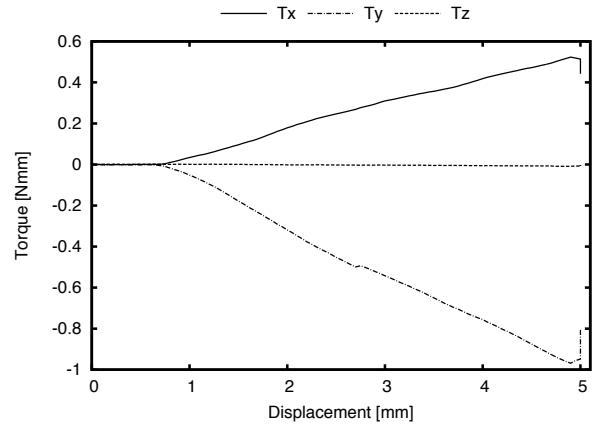


Figure B.33: 0.5 mm/s 27G - 3

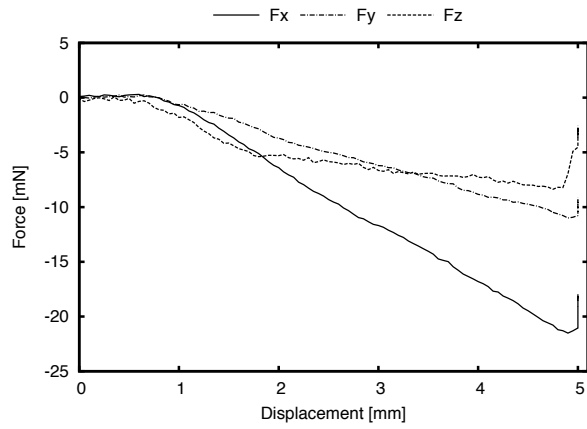


(a) Forces

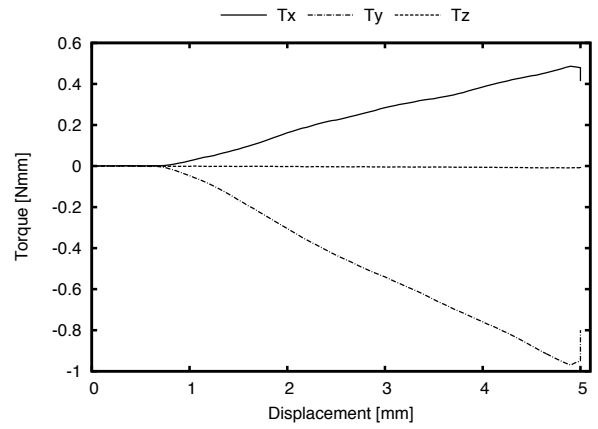


(b) Torques

Figure B.34: 0.5 mm/s 30G - 1

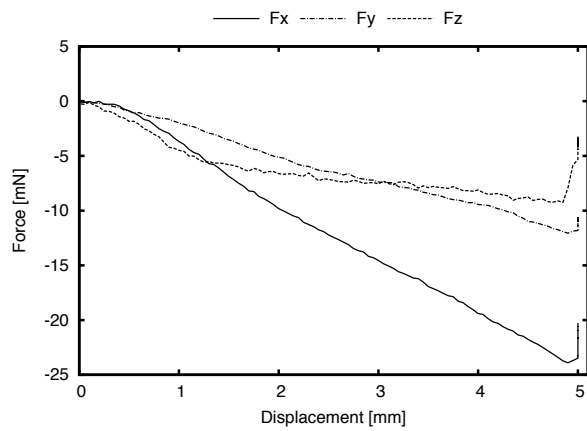


(a) Forces

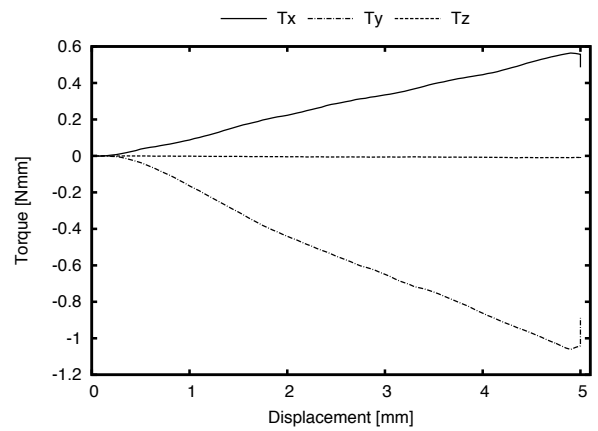


(b) Torques

Figure B.35: 0.5 mm/s 30G - 2

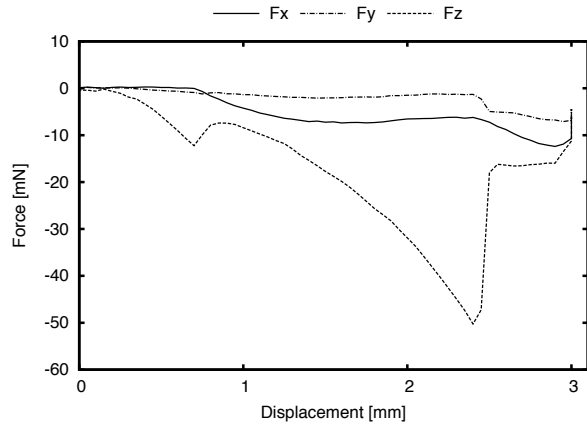


(a) Forces

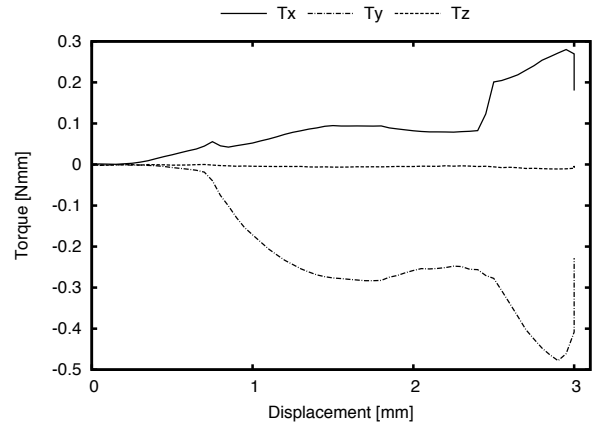


(b) Torques

Figure B.36: 0.5 mm/s 30G - 3

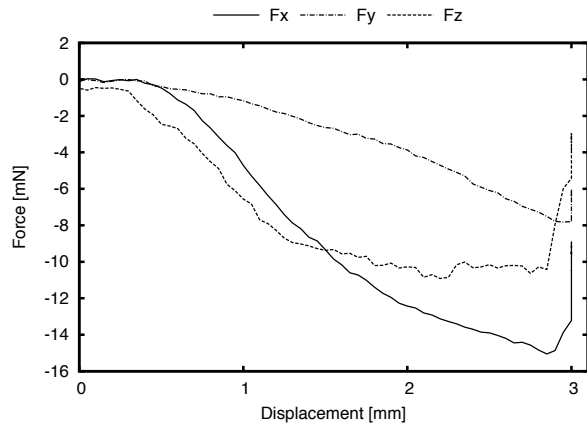


(a) Forces

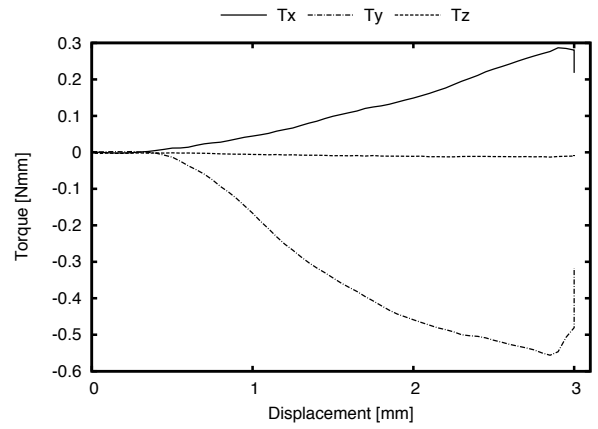


(b) Torques

Figure B.37: 0.5 mm/s *penelope* 200×400 - 1

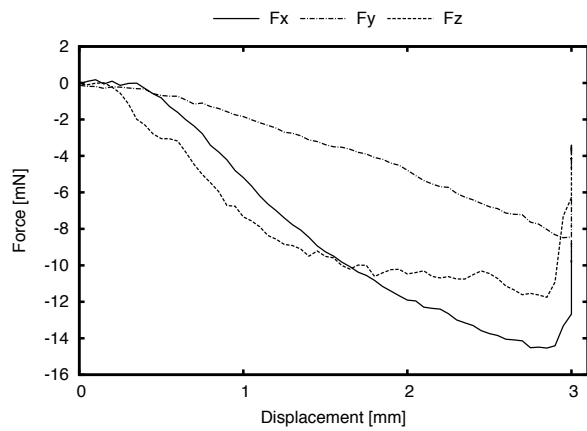


(a) Forces

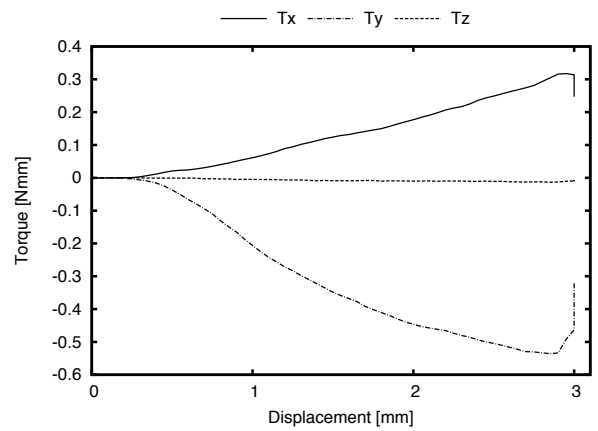


(b) Torques

Figure B.38: 0.5 mm/s *penelope* 200×400 - 2



(a) Forces



(b) Torques

Figure B.39: 0.5 mm/s *penelope* 200×400 - 3

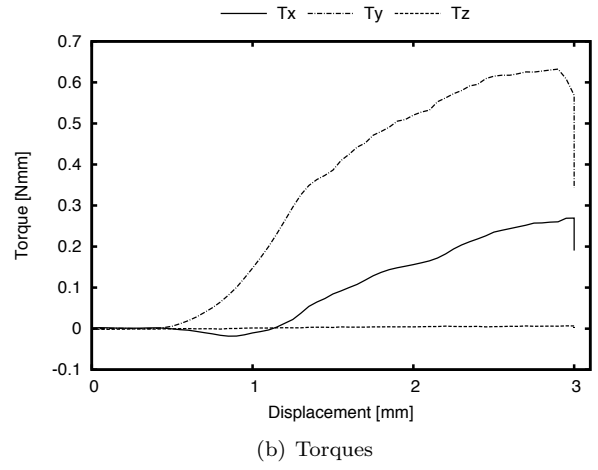
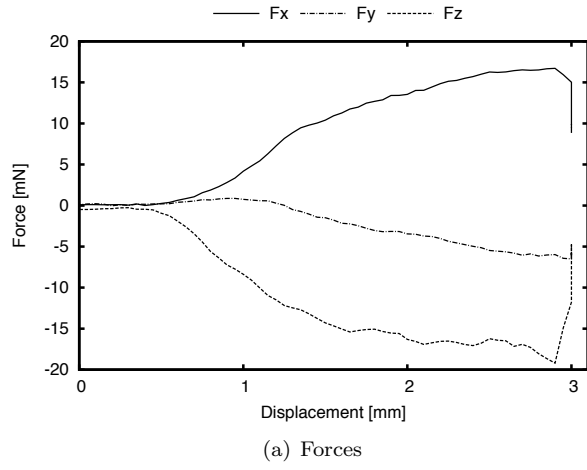


Figure B.40: 0.5 mm/s *penelope* 400×400 - 1

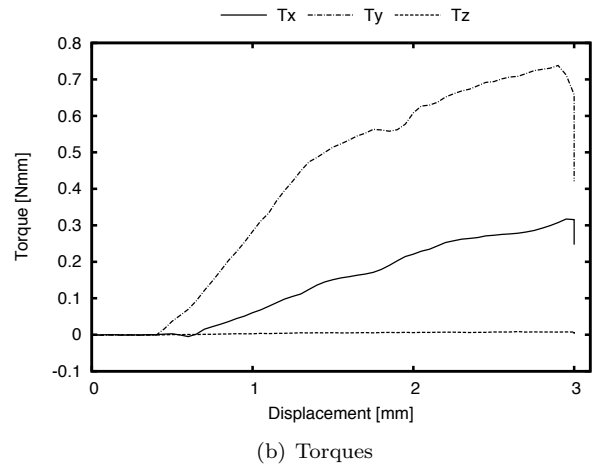
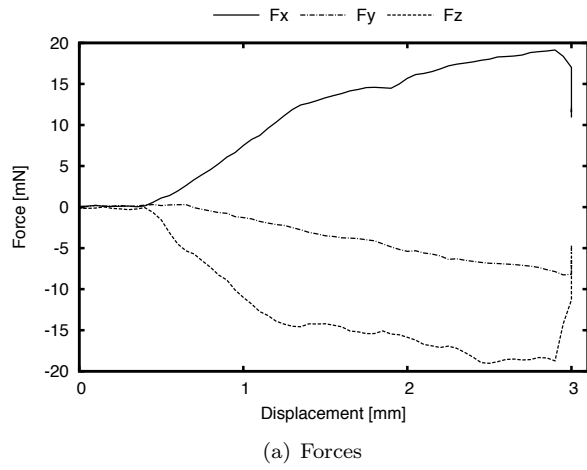


Figure B.41: 0.5 mm/s *penelope* 400×400 - 2

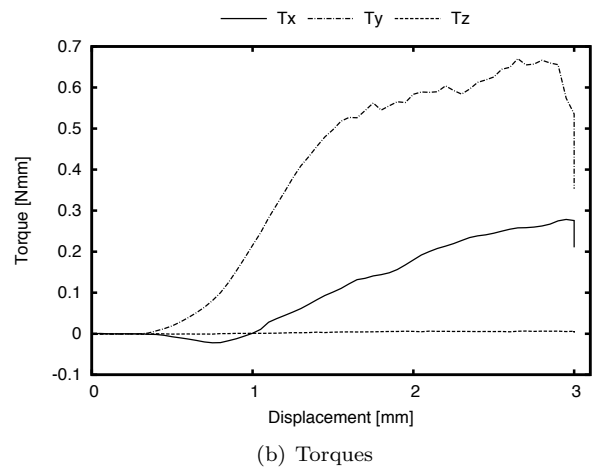
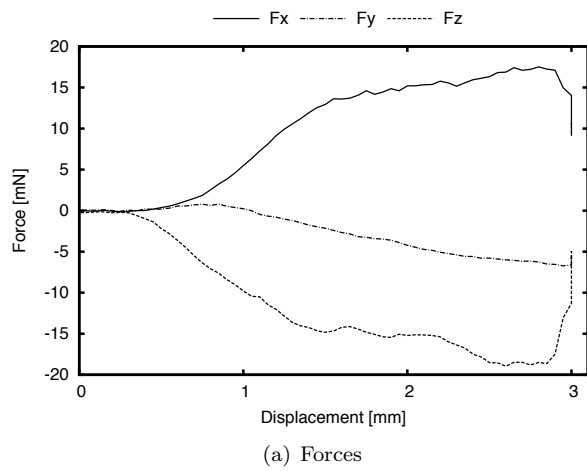
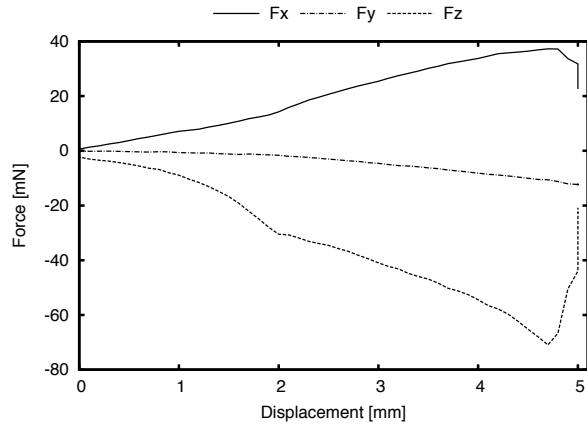
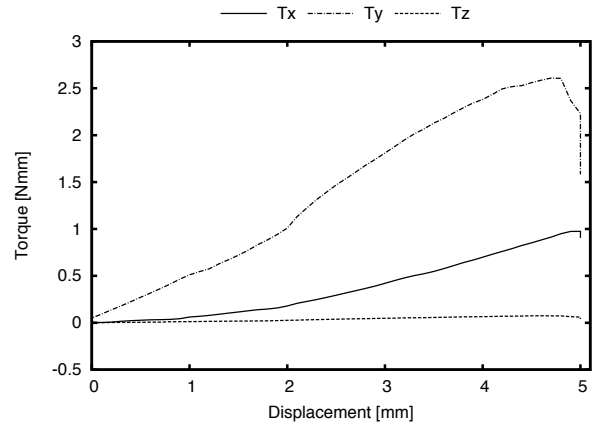


Figure B.42: 0.5 mm/s *penelope* 400×400 - 3

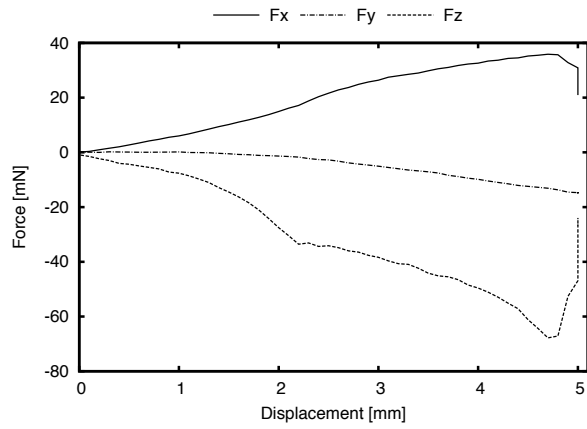


(a) Forces

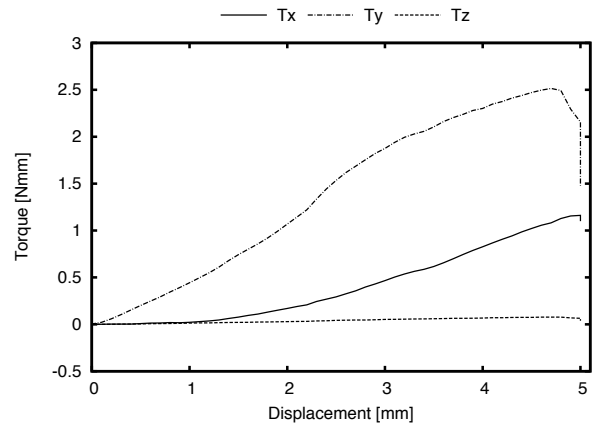


(b) Torques

Figure B.43: 1 mm/s 19G - 1

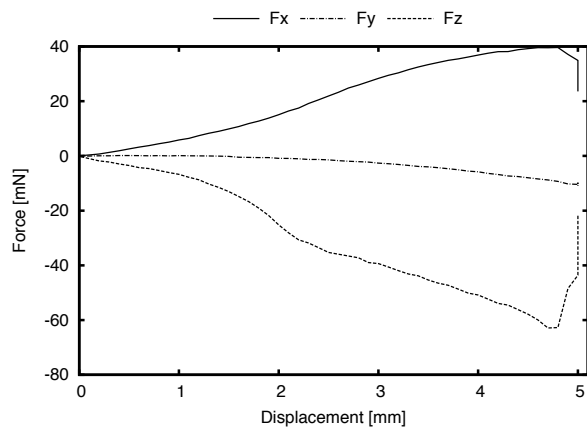


(a) Forces

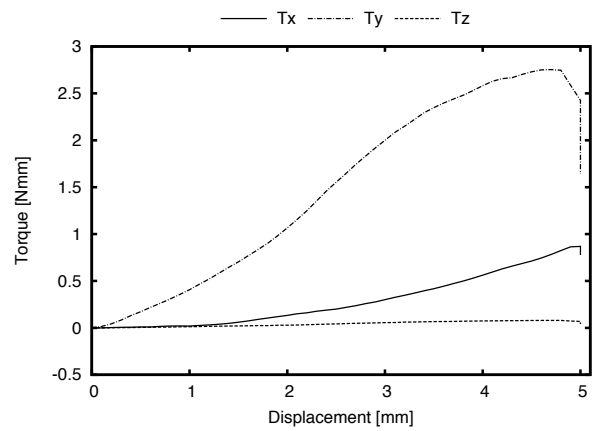


(b) Torques

Figure B.44: 1 mm/s 19G - 2

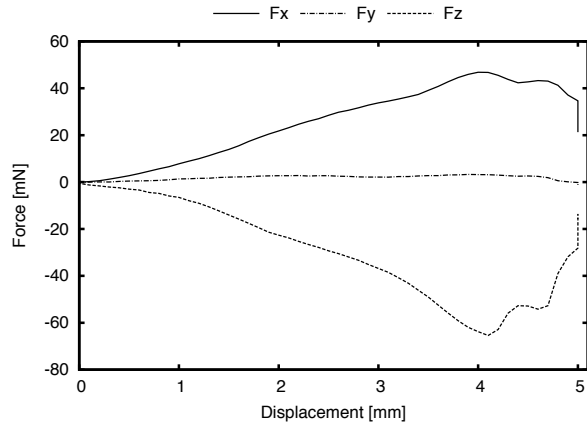


(a) Forces

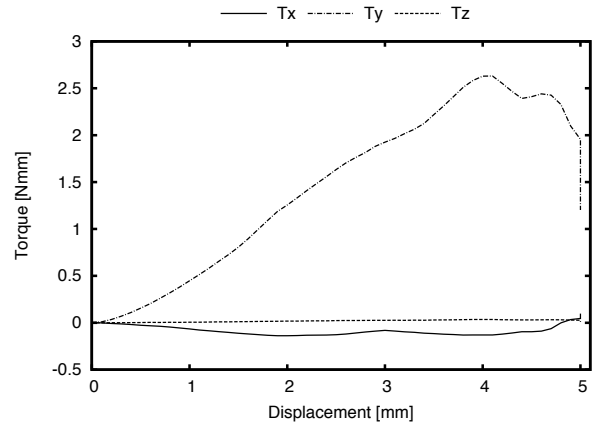


(b) Torques

Figure B.45: 1 mm/s 19G - 3

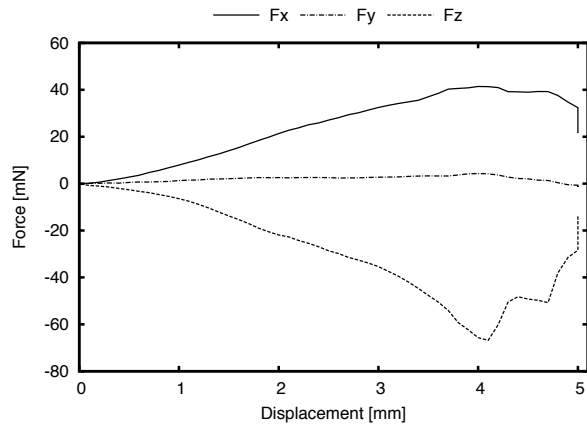


(a) Forces

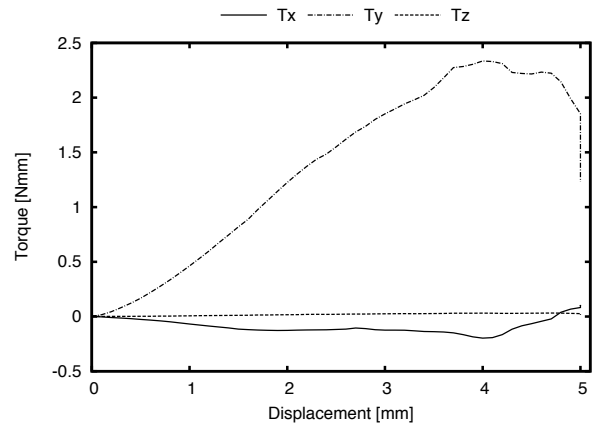


(b) Torques

Figure B.46: 1 mm/s 21G - 1

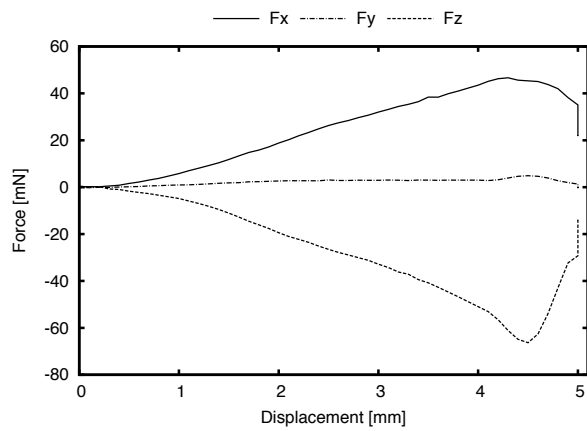


(a) Forces

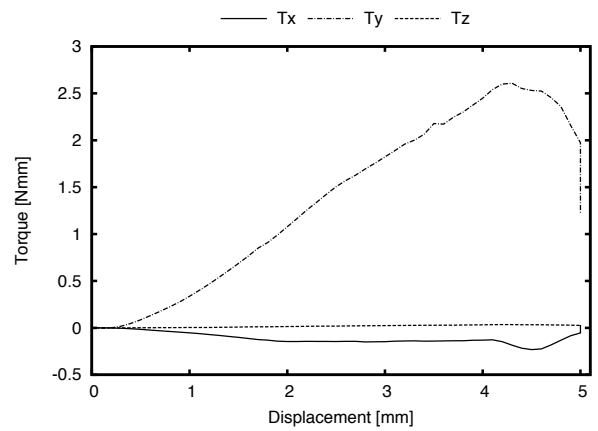


(b) Torques

Figure B.47: 1 mm/s 21G - 2



(a) Forces



(b) Torques

Figure B.48: 1 mm/s 21G - 3

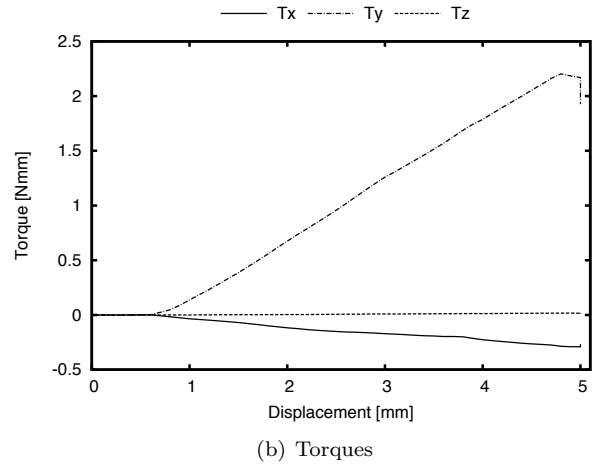
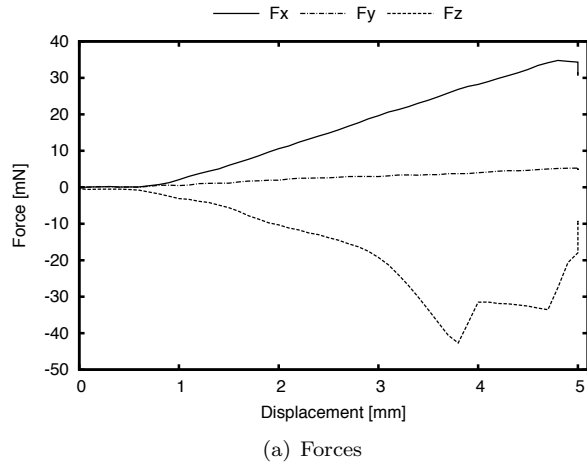


Figure B.49: 1 mm/s 23G - 1

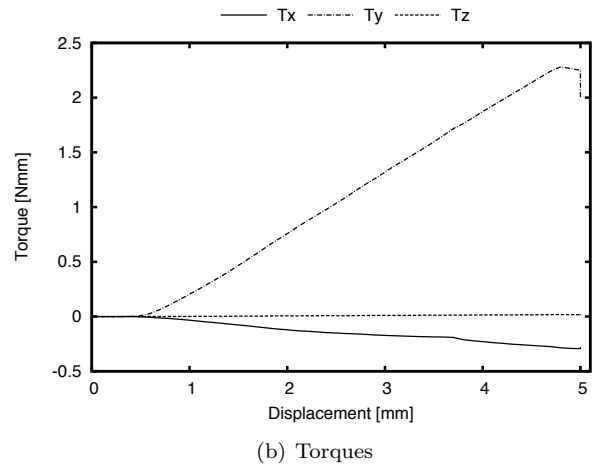
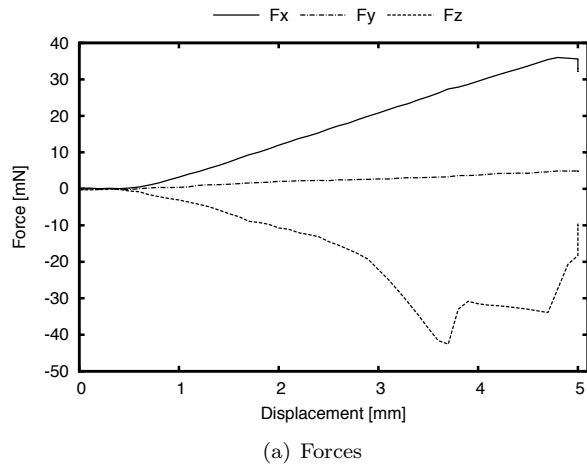


Figure B.50: 1 mm/s 23G - 2

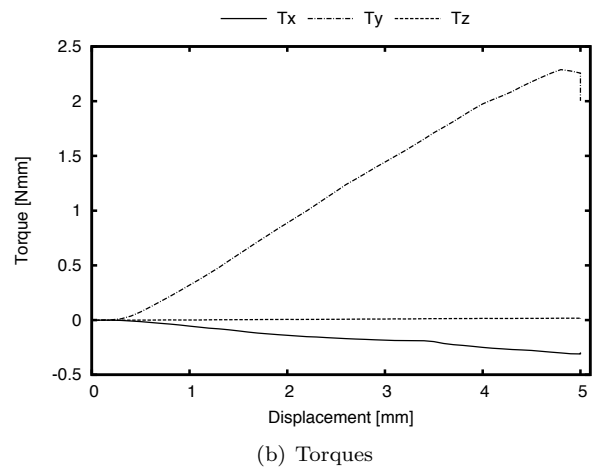
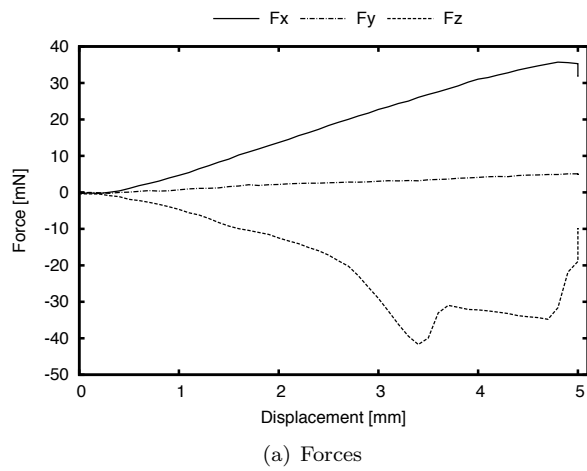


Figure B.51: 1 mm/s 23G - 3

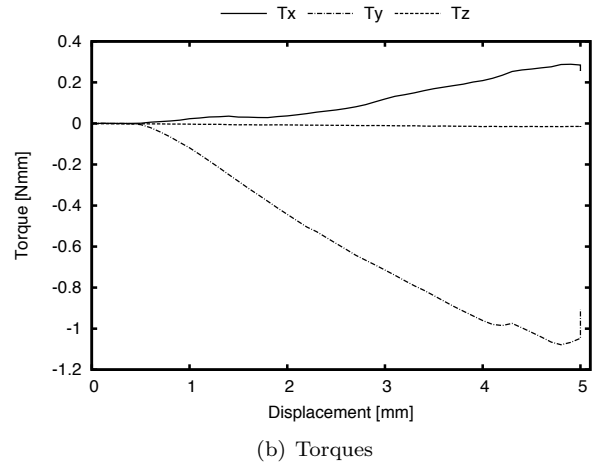
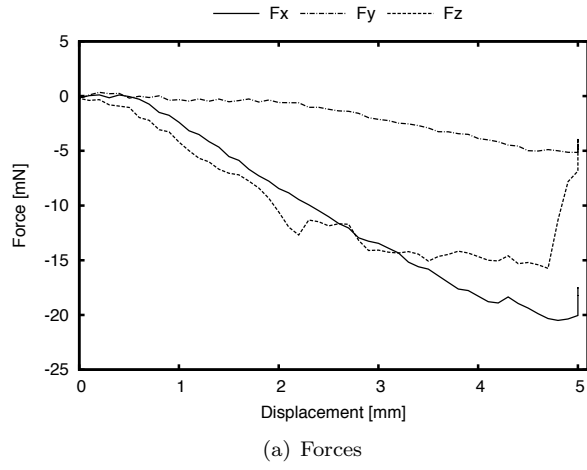


Figure B.52: 1 mm/s 27G - 1

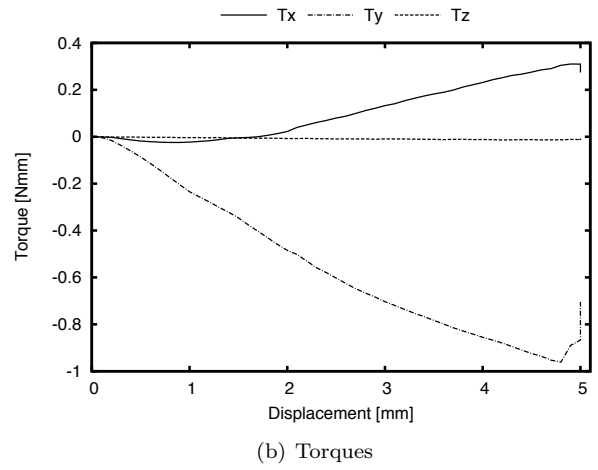
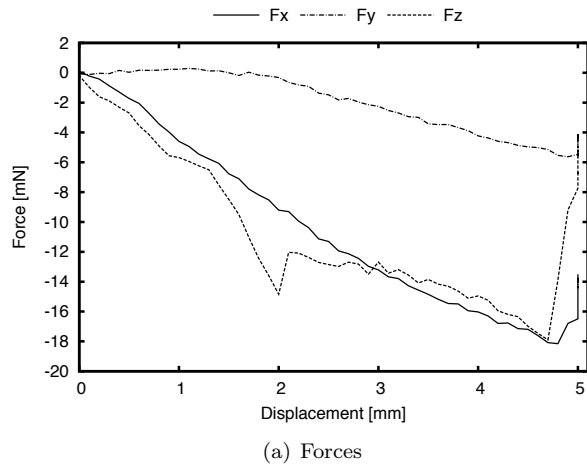


Figure B.53: 1 mm/s 27G - 2

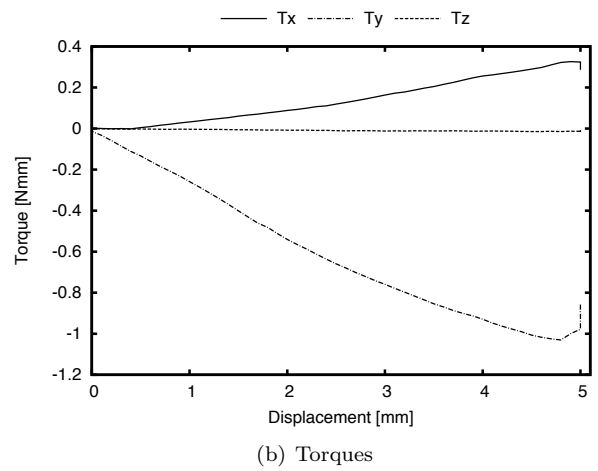
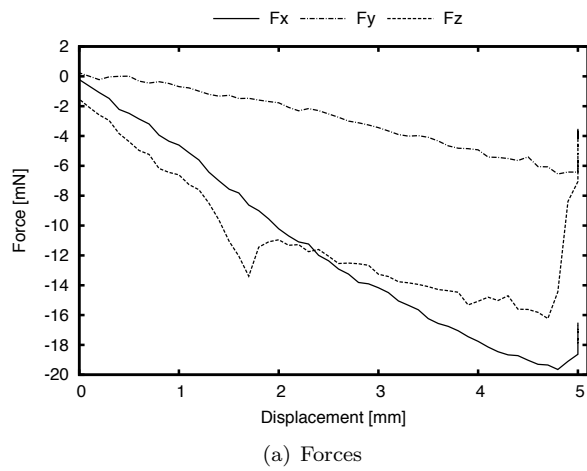


Figure B.54: 1 mm/s 27G - 3

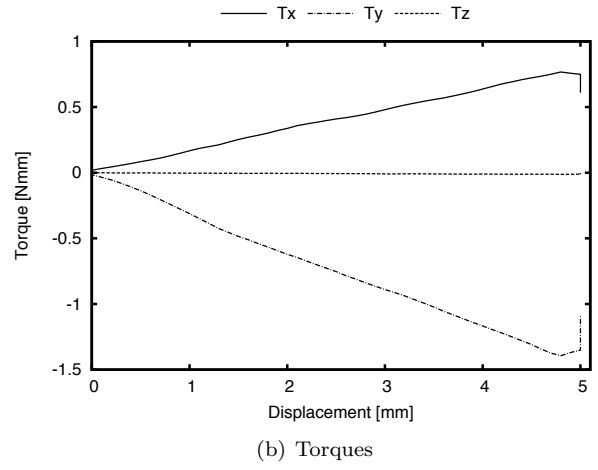
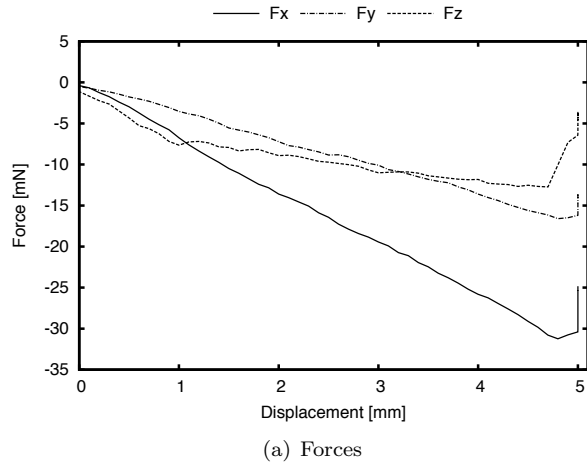


Figure B.55: 1 mm/s 30G - 1

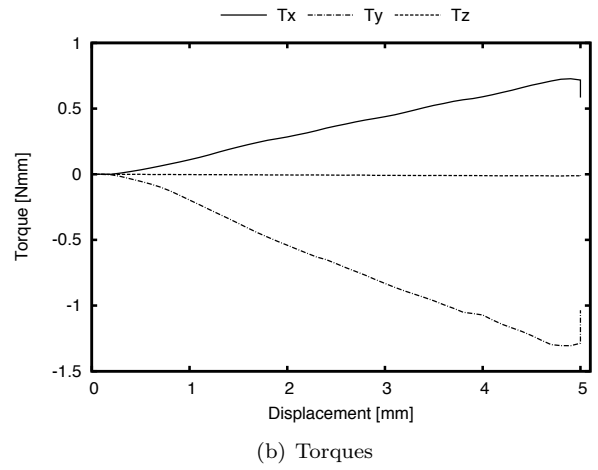
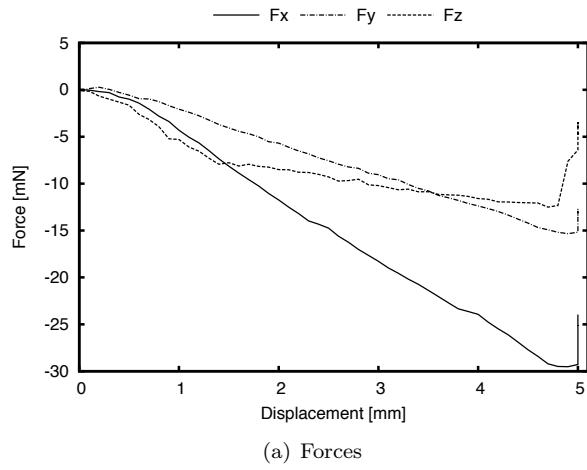


Figure B.56: 1 mm/s 30G - 2

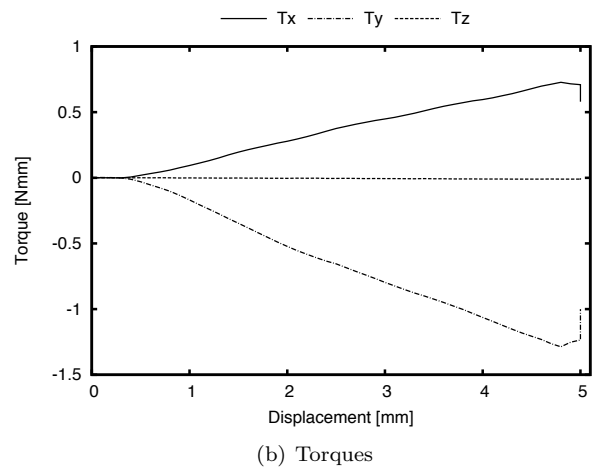
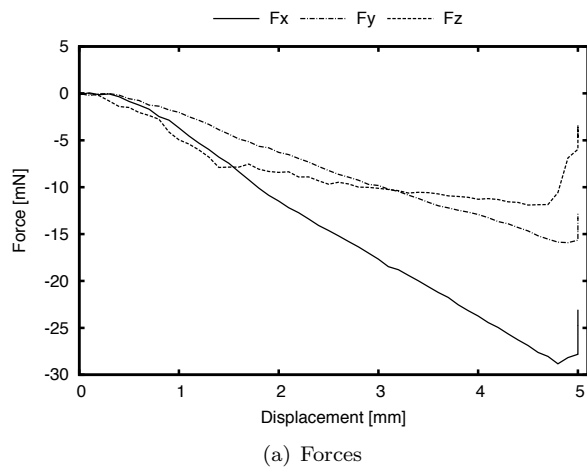
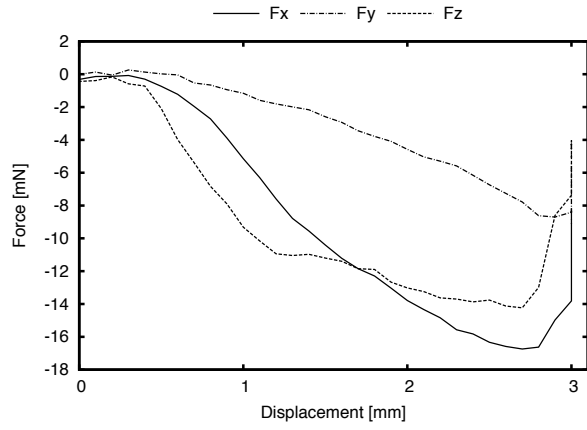
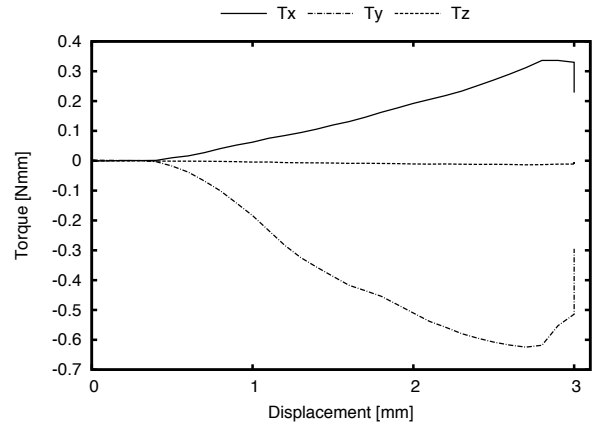


Figure B.57: 1 mm/s 30G - 3

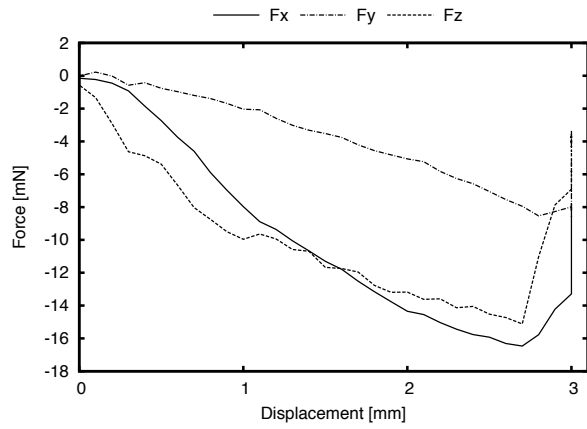


(a) Forces

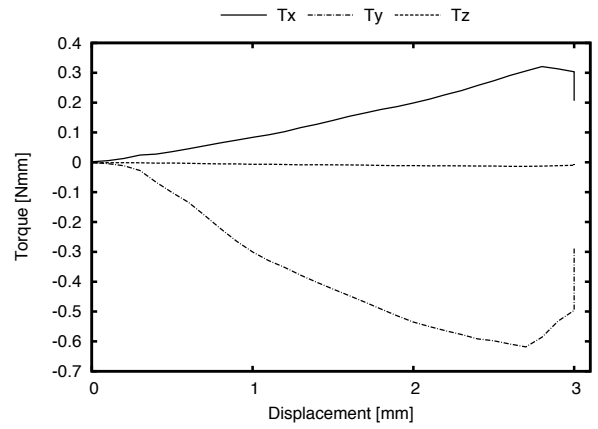


(b) Torques

Figure B.58: 1 mm/s *penelope* 200×400 - 1

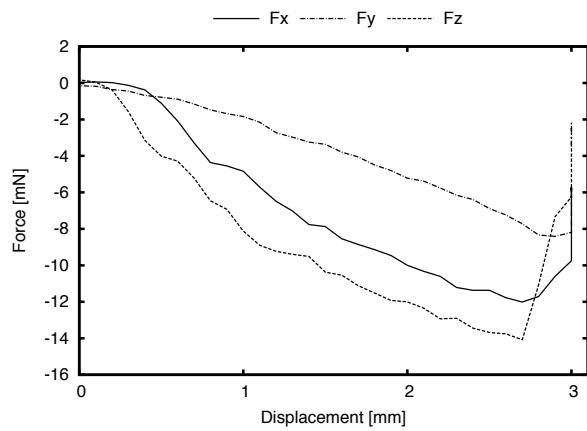


(a) Forces

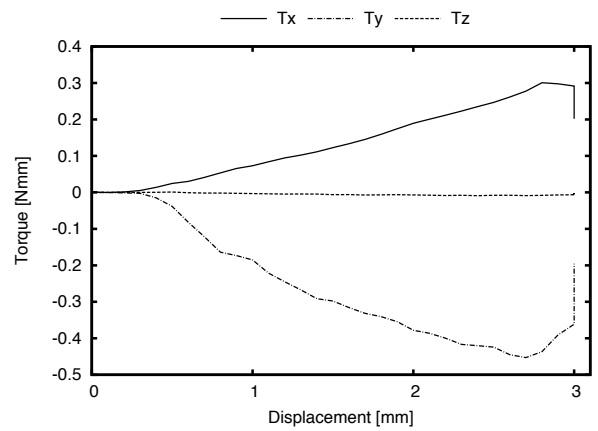


(b) Torques

Figure B.59: 1 mm/s *penelope* 200×400 - 2

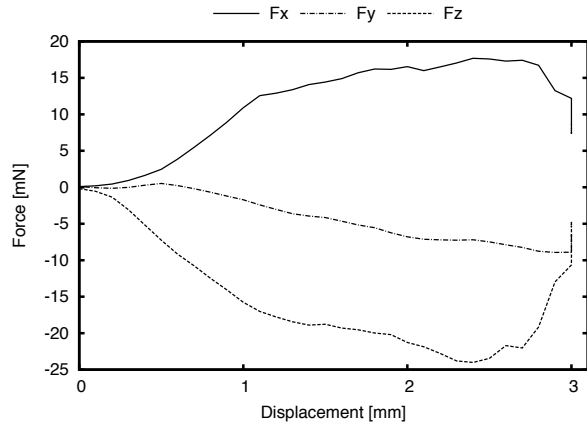


(a) Forces

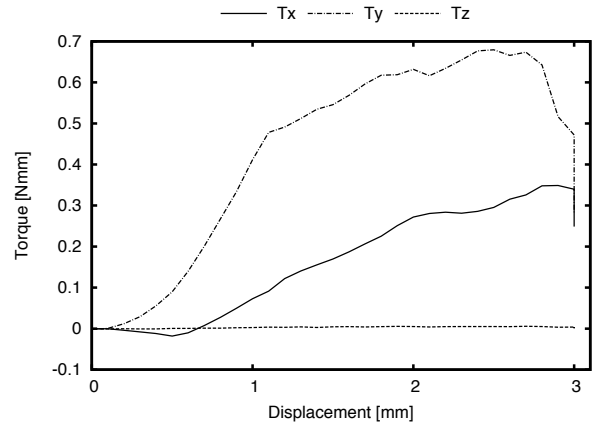


(b) Torques

Figure B.60: 1 mm/s *penelope* 200×400 - 3

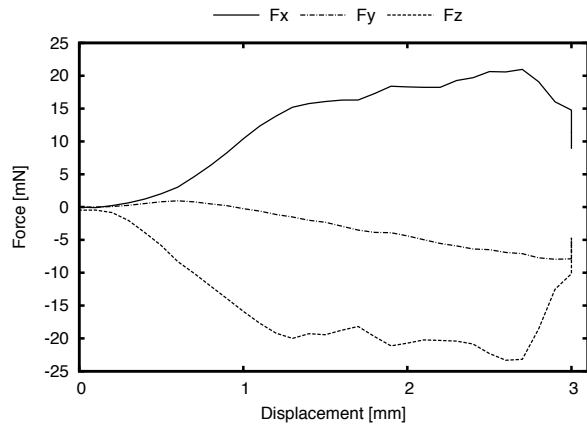


(a) Forces

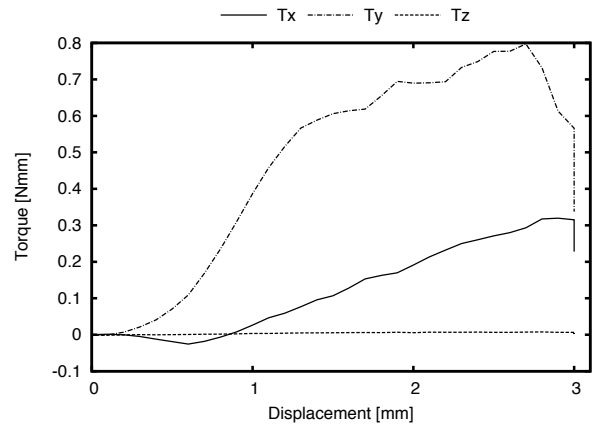


(b) Torques

Figure B.61: 1 mm/s penelope 400×400 - 1

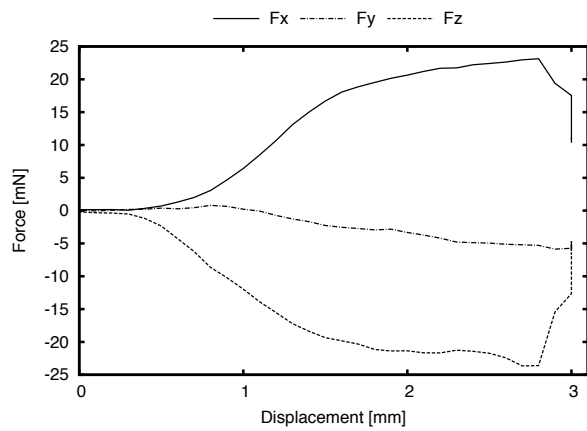


(a) Forces

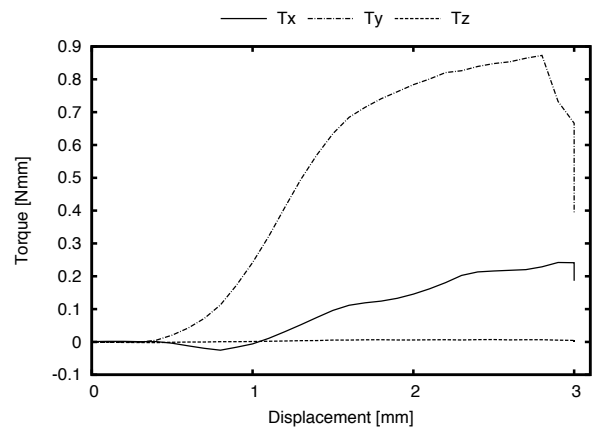


(b) Torques

Figure B.62: 1 mm/s penelope 400×400 - 2



(a) Forces



(b) Torques

Figure B.63: 1 mm/s penelope 400×400 - 3